JAERI-M
87-114

FATIGUE AND UNIAXIAL DEFORMATION BEHAVIOR OF HASTELLOY XR AT ELEVATED TEMPERATURES

August 1987

Kenji KANAZAWA*, Koji YAMAGUCHI*, Satoshi NISHIJIMA*
Isoharu NISHIGUCHI, Yasushi MUTO and Hirokazu TSUJI

日 本 原 子 力 研 究 所
Japan Atomic Energy Research Institute

JAERI-M レポートは，日本原子力研究所が不定期に公刊している研究報告書です。
入手の問合わせは，日本原子力研究所技術情報部情報資料課（〒319-11茨城県那珂郡東海村）あて，お申しこしください。なお，このほかに財団法人原子力弘済会資料センター（〒319-11 茨城県那珂郡東海村日本原子力研究所内）で複写による実費頒布をおこなっております。

JAERI-M reports are issued irregularly.
Inquiries about availability of the reports should be addressed to Information Division Department of Technical Information, Japan Atomic Energy Research Institute, Tokai-mura, Naka-gun, Ibaraki-ken 319-11, Japan.

編集兼発行　日本原子力研究所
印　　刷　いばらき印刷㈱

JAERI-M 87-114

FATIGUE AND UNIAXIAL DEFORMATION BEHAVIOR OF HASTELLOY XR AT ELEVATED TEMPERATURES

Kenji KANAZAWA*, Koji YAMAGUCHI*, Satoshi NISHIJIMA*
Isoharu NISHIGUCHI, Yasushi MUTO+ and Hirokazu TSUJI++

Department of Power Reactor Projects
Japan Atomic Energy Research Institute
Uchisaiwai-cho, Minato-ku, Tokyo

(Received July 14, 1987)

Fully reversed continuous cycling tests and tensile tests were conducted on Hastelloy XR at temperatures ranging from 600°C to 950°C in air. Fatigue life of Hastelloy XR depends on temperature. A series of SEM observation revealed that transgranular fracture with evident striation formation was dominant at temperatures below 800°C, while intergranular cracking was found above 900°C.

These results suggest that creep mechanism takes place in the fatigue behavior of this alloy above 900°C. Numerical analyses of deformation behavior during fatigue and tensile tests were conducted to interpret the experimental results. Conventional elastic-creep constitutive equation gave a good prediction of this deformation process.

Keywords: Hastelloy XR, Low Cycle Fatigue, Creep, Constitutive Equation, Striation, HTTR, Crack Propagation

+ Department of High-Temperature Engineering
++ Department of Fuels and Materials Research
* National Research Institute for Metals

JAERI－M 87－114

ハステロイXRの高温疲労特性と単軸変形挙動

日本原子力研究所動力炉開発・安全性研究管理部
金沢　健二[*]・山口　弘二[*]・西島　敏[*]
西口　磯春・武藤　康[+]・辻　宏和[++]

（1987年7月14日受理）

ハステロイXRの低サイクル疲労試験及び引張試験を大気中にて，600℃～950℃の範囲で行った。ハステロイXRの疲労特性は温度に依存する。SEMによる破面観察の結果，800℃以下ではストライエーションを伴う粒内破壊が支配的であり，900℃以上では粒界破壊が支配的であった。以上の結果から，この合金においては900℃以上の疲労挙動にはクリープの寄与が大きいことが分かった。

疲労試験および引張試験の結果を評価するために，変形挙動の数値解析を行い，従来理論に基づく弾クリープ構成方程式により変形挙動を模擬できることが分かった。

〒100東京都港区内幸町2－2－2
＋ 高温工学部
＋＋ 燃料工学部
＊ 金属材料技術研究所

Contents

1. INTRODUCTION 1
2. TEST PROCEDURES 2
2.1 Material 2
2.2 Tensile test 2
2.3 Fatigue test 2
3. TEST RESULTS 3
3.1 Tensile test 3
3.2 Fatigue test 3
4. DISCUSSIONS 4
4.1 Temperature dependence of fatigue life 4
4.2 Observation of fracture surfaces 4
4.3 Crack propagation 4
4.4 Estimation of fatigue life from tensile properties 5
4.5 Analyses of stress strain relations 6
5. CONCLUSIONS 8
REFERENCES 9

目　　次

1. 緒　　言 …… 1
2. 試験方法 …… 2
2.1 供 試 材 …… 2
2.2 引張試験 …… 2
2.3 疲労試験 …… 2
3. 試験結果 …… 3
3.1 引張試験 …… 3
3.2 疲労試験 …… 3
4. 考　　察 …… 4
4.1 疲労寿命の温度依存性 …… 4
4.2 破面観察 …… 4
4.3 き裂伝ぱ …… 4
4.4 引張特性による疲労寿命の評価 …… 5
4.5 応力－ひずみ関係の解析 …… 6
5. 結　　言 …… 8
参考文献 …… 9

1. INTRODUCTION

Development of the High-Temperature Engineering Test Reactor (HTTR) is now progressing in the Japan Atomic Energy Research Institute (JAERI). The HTTR is expected to withstand an outlet gas temperature of 950°C. This temperature is selected, as it is required for the production of hydrogen by thermo-chemical water splitting process and by steam reforming process. Therefore it must be the design temperature for internal insulation structure in piping, heat transfer tubes and tube connecting manifolds of the intermediate heat exchanger.

A nickel base heat-resistant alloy called Hastelloy XR is going to be used for these structures to cope with the very high design temperatures. This is modified Hastelloy X alloy to resist corrosion environment of HTTR helium gas[1].

In the above-mentioned structures, thermal loading is dominant due to temperature distribution in the structures both in a normal power operation and in a start-up and shut-down transient operation. It is inevitable, therefore, that cyclic thermal stresses of about 20 to 100 MPa are induced in the structural materials: low cycle fatigue under significant creep conditions would be one of the most important damaging modes. Thus detailed examination of the behavior in low cycle fatigue condition of Hastelloy XR becomes of great importance.

Low cycle fatigue tests were carried out in air at temperatures from 600°C to 950°C under a triangular strain wave form for Hastelloy XR in the National Research Institute for Metals (NRIM) as a contract research with JAERI. Tensile tests were performed in Ishikawajima-Harima Heavy Industries Co., Ltd. (IHI). This report describes the results of these test programs, where effects of temperature on fatigue and tensile properties are investigated.

A simple procedure proposed by Manson[2] is adopted to estimate fatigue life. Stress-strain relation, namely, constitutive relation under cyclic loading is discussed from the viewpoint of structural design.

2. TEST PROCEDURES

2.1 Material

Chemical composition and microphotographs of Hastelloy XR used are given in Table 1 and Fig. 1, respectively. The material was subjected to solution treatment at 1180°C for 50 min followed by rapid cooling. ASTM grain size number of this material was 4.

2.2 Tensile test

Tensile tests were accomplished using specimens with 6 mm in diameter and 30 mm in gage length. They were conducted at room temperature and over the temperatures ranging from 600°C to 950°C at every 50°C in air, using the test procedures described in JIS G0567[3]. Strain rate was kept at 0.3 %/min until 0.2 % proof stress was observed and then switched to 10 %/min in cross head speed.

2.3 Fatigue test

Low cycle fatigue tests were conducted on electro-hydraulic fatigue testing machines. Profile of specimens are shown in Fig. 2. Temperature of specimens was monitored by thermocouples. Deviation of temperature from the aimed temperature was controlled within 5°C.

Total axial strain was controlled by using an extensometer, whose 2 tips of quartz glass bars were attached to the parallel gage section of the specimens. Fatigue tests under fully reversed triangular wave form were carried out at a strain rate of 0.1 %/s in air at temperatures of 600, 800, 850, 900 and 950°C.

3. TEST RESULTS

3.1 Tensile test

Tensile properties of Hastelloy XR are given in Table 2. Figure 3 shows temperature dependence of 0.2 % proof stress and tensile strength. Variation of fracture elongation and reduction in area are shown in Figs. 4 and 5, respectively.

Figure 6 shows nominal stress - nominal strain curves obtained. Appearances of tensile specimens tested are shown in Fig. 7.

3.2 Fatigue test

a) Fatigue life

Table 3 shows fatigue test results obtained in this test program. Definitions of stress range $\Delta\sigma$, total strain range $\Delta\varepsilon_t$, plastic strain range $\Delta\varepsilon_p$ and elastic strain range $\Delta\varepsilon_e$ are shown in Fig. 8. Cycles to failure Nf is defined as the number of cycles to complete separation of the specimen into two parts. $\Delta\sigma$ in the table is the value at a cycle about 1/2Nf. Plots of total strain range, plastic strain range and elastic strain range vs. cycles to failure are given in Fig. 9. In the figure, regression curves are given as follows:

$$\Delta\varepsilon_e = CeNf^{ke} \tag{1}$$

$$\Delta\varepsilon_p = CpNf^{kp} \tag{2}$$

$$\Delta\varepsilon_t = \Delta\varepsilon_e + \Delta\varepsilon_p = CeNf^{ke} + CpNf^{kp} \tag{3}$$

where exponents and coefficients of the equations are summarized in Table 4.

b) Variation of stress range

Figure 10 shows variation of stress range during cyclic straining. It can be seen that Hastelloy XR shows cyclic strain hardening behavior at 600°C, but the change in stress range during testing decreases at test temperatures above 900°C. The dependence of stress range on the total strain range decreases with increasing test temperature. This can be seen more apparently on cyclic stress strain curves shown in Fig. 11, based on values at 1/2Nf, where monotonic stress-strain curves of tensile tests are shown also.

4. DISCUSSIONS

4.1 Temperature dependence of fatigue life

Figures 12, 13 and 14 show $\Delta\varepsilon_t$-Nf, $\Delta\varepsilon_e$-Nf and $\Delta\varepsilon_n$-Nf relationships, respectively. In $\Delta\varepsilon_e$-Nf relationship, fatigue life decreased with increasing temperature. The temperature dependence of $\Delta\varepsilon_e$-Nf relationship is more remarkable than that of $\Delta\varepsilon_p$-Nf relationship. Temperature insensitivity of $\Delta\varepsilon_p$-Nf relationship has been pointed out for Hastelloy X[4].

Figure 15 shows $\Delta\varepsilon_t$-Nf relationship of Hastelloy X and XR of references (4), (5), (6) with the present data. There is no clear difference between them.

4.2 Observation of fracture surfaces

Figure 16 shows microphotographs of the fracture surface of the fatigued specimens. Evident striations were observed at the specimens fatigued at 600 and 800°C. For the specimens fatigued at 850°C, intergranular facets were observed at the limited region near the specimen surface but the transgranular fracture mode was dominant as a whole. On the other hand, the intergranular fracture mode was dominant at 900 and 950°C.

Figure 17 shows fatigue cracks observed at the cross section of the specimens fatigued at 600 and 800°C, where typical striations were formed as stated above.

4.3 Crack propagation

As each striation is formed at every strain cycle, it is possible to know the crack propagation rate dl/dn by measuring the spacing of the striations. The relation between dl/dn and the crack length l (mm) is shown in Fig. 18. The crack propagation rate is expressed as follows:

$$dl/dn = A\, l^{\gamma} \qquad (4)$$

where A and γ are constants which depend on test conditions and materials. The value of A gives the crack propagation rate at a crack length of 1 mm. Four values of A obtained from Fig. 18 for Hastelloy XR

are plotted in Fig. 19 with the data of austenitic stainless steels obtained at room temperature, 450°C, 600°C and 700°C[7]. The value of γ is about 1.3 for both materials of Hastelloy XR and austenitic stainless steels. These results suggest that the crack propagation mechanism of Hastelloy XR at temperature below 800°C would be the same as that of austenitic stainless steels.

4.4 Estimation of fatigue life from tensile properties

Manson proposed the universal slope method to estimate the low cycle fatigue life from the results of tensile tests[2]. According to the method, the relation between the total strain range and the fatigue life is given by

$$\Delta\varepsilon_t = (3.5\ \sigma_B/E)Nf^{-0.12} + D^{0.6}\ Nf^{-0.6} \qquad (I)$$

where the unit of strain is mm/mm and

σ_B : tensile strength (MPa)
E : Young's modulus (MPa)
D : fracture ductility evaluated from the reduction in area as $\ln(100/(100-\psi))$
ψ : reduction in area (%)

In equation (I), the first term gives the elastic strain range $\Delta\varepsilon_e$ as a function of tensile strength and the second term gives the plastic strain range $\Delta\varepsilon_p$ as a function of fracture ductility.

For high temperature tests, equation (I) is modified as

$$\Delta\varepsilon_t = (3.5\ \sigma_B/E)(5Nf)^{-0.12} + D^{0.6}(5Nf)^{-0.6} \qquad (II)$$

or in the case of creep effect and oxidation effect being remarkable, it is modified as

$$\Delta\varepsilon_t = (3.5\ \sigma_B/E)(10Nf)^{-0.12} + D^{0.6}(10Nf)^{-0.6} \qquad (III)$$

In equations (II) and (III), fatigue lives are estimated as 1/5 and 1/10 in comparison with life by equation (I), respectively.

Equation (I) is written for Hastelloy XR at each test temperature as follows:

$$\Delta\varepsilon_t = 1.21Nf^{-0.12} + 85Nf^{-0.6} \quad \text{at } 600°C \tag{5}$$

$$\Delta\varepsilon_t = 0.89Nf^{-0.12} + 122Nf^{-0.6} \quad \text{at } 800°C \tag{6}$$

$$\Delta\varepsilon_t = 0.73Nf^{-0.12} + 135Nf^{-0.6} \quad \text{at } 850°C \tag{7}$$

$$\Delta\varepsilon_t = 0.59Nf^{-0.12} + 134Nf^{-0.6} \quad \text{at } 900°C \tag{8}$$

$$\Delta\varepsilon_t = 0.47Nf^{-0.12} + 132Nf^{-0.6} \quad \text{at } 950°C \tag{9}$$

where the unit of strain is %. The curves for these equations and equations (II) and (III) are shown in Fig. 20 with the fatigue test data. It can be seen that test data lie between equations (I) and (II) at 600°C and between equations (II) and (III) at test temperatures above 800°C. Lives estimated by the Manson's method are compatible with the experimental results.

4.5 Analyses of stress strain relations

The result of SEM observation suggests that typical creep effect is contained in the fatigue behavior at the strain rate of 0.1 %/s at temperatures above 900°C. The change in the stress range during cyclic straining also shows different tendency around this temperature. Hastelloy XR shows strain hardening behavior at 600°C, but the change in the stress range decreases as the test temperature increases. The stress range is almost stationary at temperatures above 900°C. The dependence of the stress range on the total strain range decreases, too. It is probable that the stress range is not determined only from the strain range without knowing the strain rate, as the creep effect is significant.

To examine this observation, numerical analyses of monotonic and cyclic deformation behavior were performed for fatigue and tensile tests data, respectively, using elastic-creep constitutive equation. Creep equation of Hastelloy X[8] was used in the analyses where creep strain ε_c is expressed by Garofalo's equation, as

$$\varepsilon_c = \varepsilon_1 (1 - e^{-rt}) + \dot{\varepsilon}_{min,t} \tag{10}$$

where ε_1 : primary creep strain

$\dot{\varepsilon}_{min}$: minimum creep strain rate
t : time
r : coefficient depending on stress

The results obtained were as folows:

a) Montonic behavior

Figure 21 shows nominal stress vs. nominal strain relation obtained by FEM model where finite deformation theory[9] in which the co-rotational rate of Kirchhoff stress and the rate of deformation are used and strain hardening rule is taken into consideration. Good agreement is obtained between numerical analysis and experimental results at 900°C and 950°C. It should be noted that plastic strain is not considered in numerical analyses and only elastic and creep effects are assumed. Decrease of nominal stress succeeding to the peak stress is a result of adopting finite deformation theory.

b) Cyclic behavior

Cyclic behavior was simulated using the same constitutive equation. Calculated stress during cyclic straining is shown with the experimental result in Fig. 22. Figure 23 shows the hysteresis loops where small strain theory is adopted. The values of calculated stress amplitude are 222 MPa and 172 MPa at 900 and 950°C, respectively, for a strain range of 0.5%. These values are somewhat larger than those of the test results shown in Fig. 10.

Numerical analysis was done also for temperatures below 850°C, but good accordance with the experimental results was not obtained. The results are consistent with the anticipation that creep effect is remarkable in the fatigue and tensile tests at temperatures above 900°C under the strain rate of 0.1 %/s, in the present work. Similar strain rate dependency is pointed out also for Inconel 617[10] for tensile properties at elevated temperatures.

From the viewpoint of structural design, it may be said that at temperatures above 900°C, the constitutive equation where elastic and creep deformation mechanisms were assumed, would be enough valid for broader loading conditions up to a strain rate of 0.1 %/s.

5. CONCLUSIONS

Fully reversed continuous cycling tests were conducted on Hastelloy XR at temperatures ranging from 600 to 950°C in air at a strain rate of 0.1 %/s. Conclusions obtained in these tests as follows:

(1) Hastelloy XR showed almost the same fatigue life properties as those of Hastelloy X.

(2) Fatigue life of Hastelloy XR depends on the temperature condition and fatigue life decreased as temperature increased. The temperature dependence of $\Delta\varepsilon_e$-Nf relationship was more remarkable than that of $\Delta\varepsilon_p$-Nf relationship.

(3) A series of SEM observations revealed that the transgranular fracture mode with the evident striation formation was dominant at temperatures below 800°C, and intergranular cracking above 900°C.

(4) The change in the stress range during cyclic straining showed different tendency at these temperature ranges. Hastelloy XR showed cyclic strain hardening behavior at 600°C, but the change in stress range during cyclic straining decreased with increasing test temperature. The dependence of stress range on the total strain range disappeared. These results suggest that creep effect plays an important role in the fatigue process for temperatures above 900°C at a strain rate of 0.1 %/s.

(5) Numerical analyses of deformation behavior during fatigue and tensile tests were conducted to interpret the experimental results.
Conventional elastic-creep constitutive equation gave a good prediction of this deformation process.

REFERENCES

(1) M. Shindo and T. Kondo, Proceeding of British Nuclear Energy Society Conference, Bristol (1982).

(2) S.S. Manson, "A simple procedure for estimating high-temperature low-cycle fatigue", Experimental Mechanics, vol.8, pp349-355 (1968).

(3) Japanese Industrial Standard, "Method of high temperature tensile test for steels and heat-resisting alloys (JIS G 0567)".

(4) S. Shimizu et al., "High temperature low-cycle fatigue strength of Hastelloy X", Zairyo, vol.26, pp.255-261 (1977), (in Japanese).

(5) H. Tsuji and T. Kondo, "Low-cycle fatigue of Hastelloy X and Hastelloy XR in simulated VHTR helium coolant environment at elevated temperature", JAERI-M 84-014 (1984).

(6) Brinkman et al., "Application of Hastelloy X in gas-cooled reactor systems", ORNL TM-5405 (1976).

(7) K. Yamaguchi and K. Kanazawa, "Crack propagation rates of austenitic stainless steels under high-temperature low-cycle fatigue conditions", Metallurgical Transcations A, vol.10A, pp.1445-1451 (1979).

(8) K. Suzuki and Y. Mutoh, "Study on the creep constitutive equation of Hastelloy X", Bulletin of JSME, vol.26, No.221 (1976).

(9) R.M. McMeeking and J.R. Rice, "Finite-element formulations for problems of large elastic-plastic deformation", Int. J. Solids Structures, vol.11, pp.601-616 (1975).

(10) M. Kitagawa et al., "Some problems in developing the high temperature design code for a 1.5 MWt helium heat exchanger", 1976 Elevated Temperature Design Symposium, ASME, Mexico City, pp.33-40 (1976).

Table 1 Chemical composition of Hastelloy XR used

wt.%

C	Mn	Si	P	S	Cr	Co	Mo	W	Fe	B	Al	Ti	N
0.08	0.95	0.30	0.005	0.001	22.03	0.06	9.17	0.46	18.24	0.001	0.05	0.05	0.001

Table 2 Tensile test results

Temperature (°C)	Yield stress (MPa)	Tensile stress (MPa)	Elongation (%)	Reduction in area (%)
R.T.	325	716	49.0	60.0
	323	712	48.7	60.6
	323	712	49.0	60.2
600	212	540	53.3	53.6
	212	542	52.0	50.7
650	203	531	50.3	49.6
	203	532	50.3	57.0
700	205	482	55.7	54.7
	203	484	53.0	58.6
750	196	424	58.7	66.3
	200	420	50.7	67.1
800	196	363	63.3	75.5
	203	365	56.0	74.7
850	175	295	61.7	80.6
	179	290	64.7	80.7
900	129	223	61.0	80.3
	130	228	65.3	80.0
950	98	177	67.3	78.4
	96	176	71.0	80.6

Table 3 Fatigue test results

Temperature (°C)	$\Delta\varepsilon_t$ (%)	$\Delta\varepsilon_p$ (%)	$\Delta\varepsilon_e$ (%)	$\Delta\sigma$ (MPa)	N_f
600	1.33	0.68	0.65	1091	577
	1.05	0.43	0.62	988	894
	0.80	0.23	0.57	952	1819
	0.70	0.18	0.52	884	2599
	0.69	0.12	0.57	906	4636
	0.55	0.06	0.49	808	8434
	0.50	0.04	0.46	787	18016
800	1.04	0.64	0.40	586	560
	0.71	0.37	0.34	547	1138
	0.66	0.31	0.35	544	1088
	0.49	0.19	0.30	500	2193
	0.42	0.11	0.31	466	4202
	0.34	0.06	0.28	426	18803
	0.33	0.04	0.29	422	31428
850	1.92	1.57	0.35	491	290
	0.98	0.69	0.29	455	710
	0.69	0.42	0.27	446	1250
	0.48	0.24	0.24	409	2060
	0.39	0.10	0.29	350	5807
	0.30	0.06	0.24	299	16396
900	1.94	1.67	0.27	365	163
	0.99	0.72	0.27	343	930
	0.69	0.46	0.23	352	1450
	0.49	0.29	0.20	377	1708
	0.40	0.19	0.21	346	3584
	0.31	0.10	0.21	334	5832
950	1.94	1.73	0.21	273	229
	0.98	0.79	0.19	259	890
	0.70	0.52	0.18	284	1285
	0.49	0.32	0.17	268	2922
	0.40	0.23	0.17	289	4092
	0.30	0.12	0.18	293	5436

Table 4 Exponents and coefficients of regression curves

Temperature (°C)	$\Delta\varepsilon_t = \Delta\varepsilon_e + \Delta\varepsilon_p = C_e N_f^{ke} + C_p N_f^{kp}$			
	Ce	ke	Cp	kp
600	1.18	−0.096	124.	−0.829
800	0.576	−0.072	33.5	−0.655
850	0.472	−0.070	157.	−0.831
900	0.424	−0.084	109.	−0.780
950	0.286	−0.061	142.	−0.786

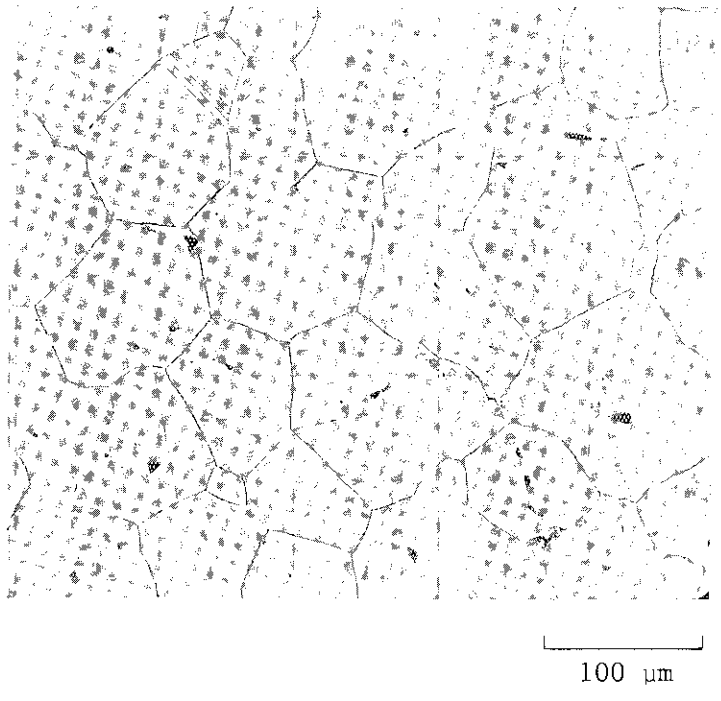

Fig. 1 Microphotograph of Hastelloy XR used

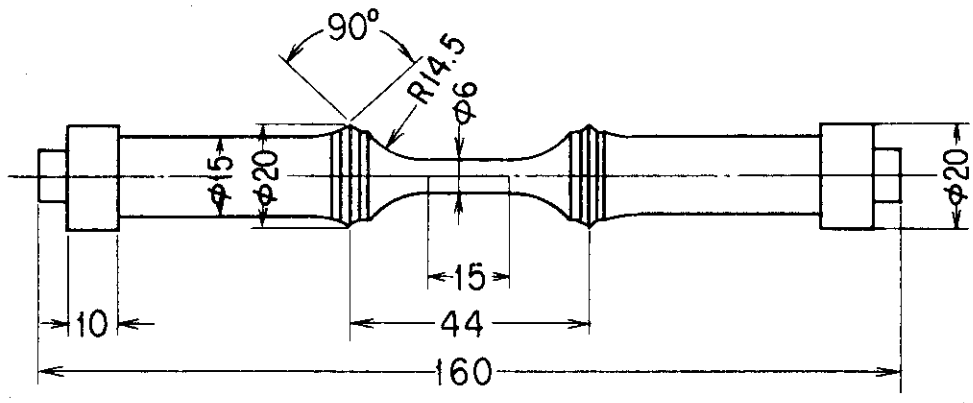

for tests at 600 ℃ and 800 ℃

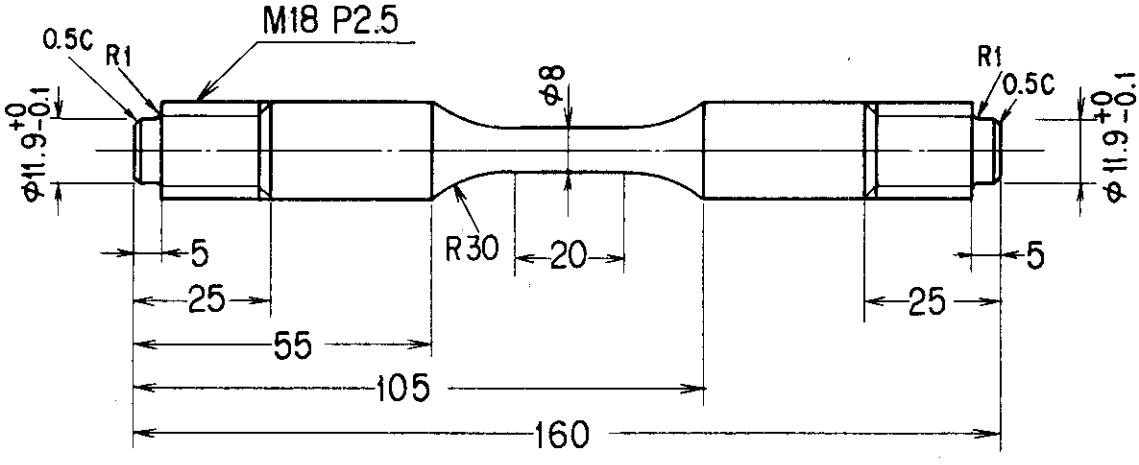

for tests at 850, 900 and 950 ℃

Fig. 2 Fatigue test specimens

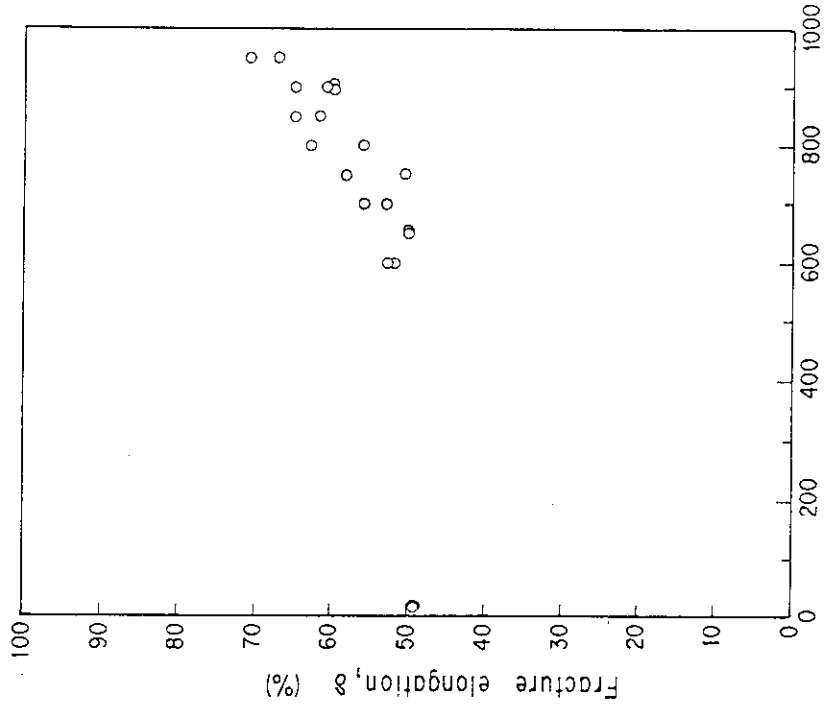

Fig. 4 Fracture elongation vs. temperature

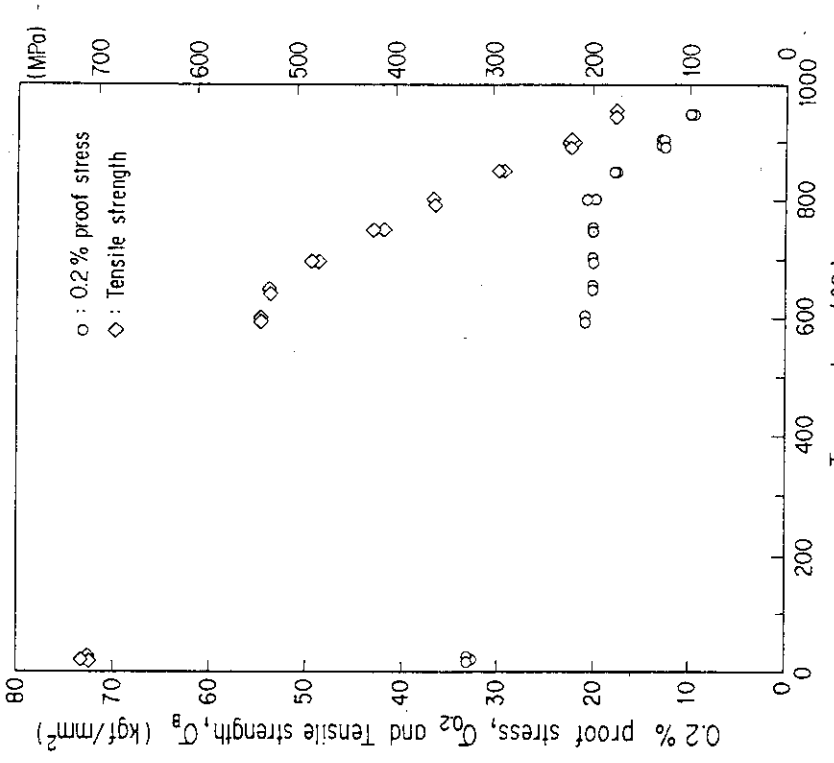

Fig. 3 0.2 % proof stress and tensile strength vs. temperature

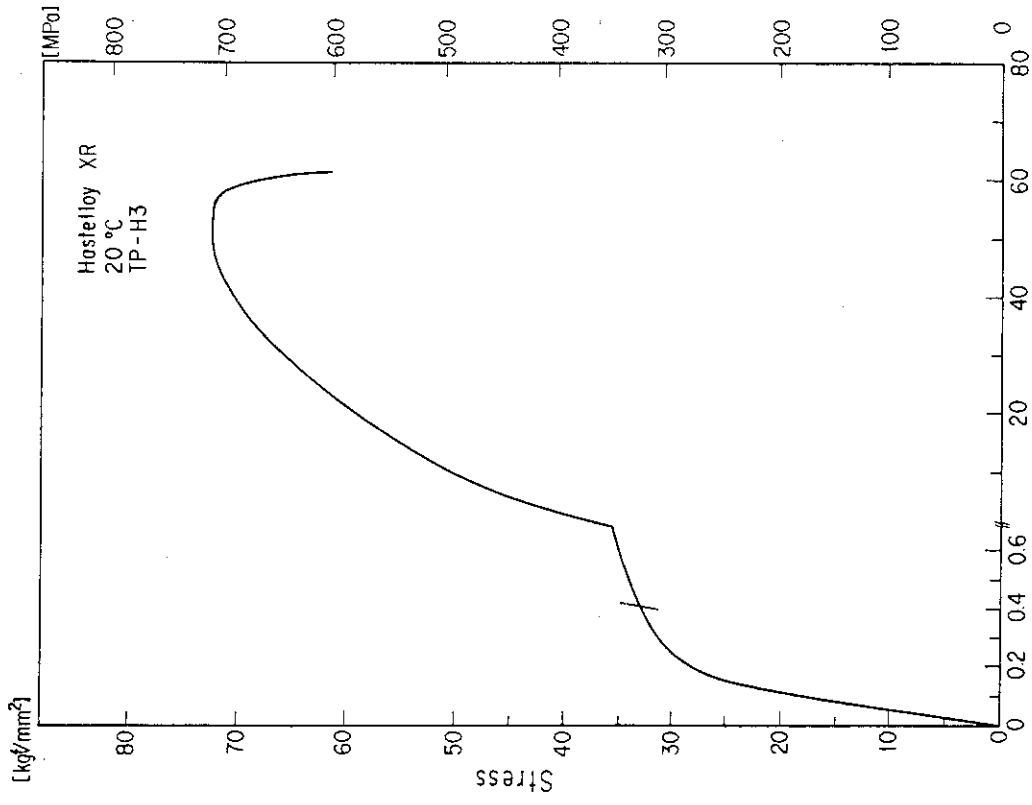

(a) Tested at room temperature

Fig. 6 Tensile stress-strain curves of Hastelloy XR

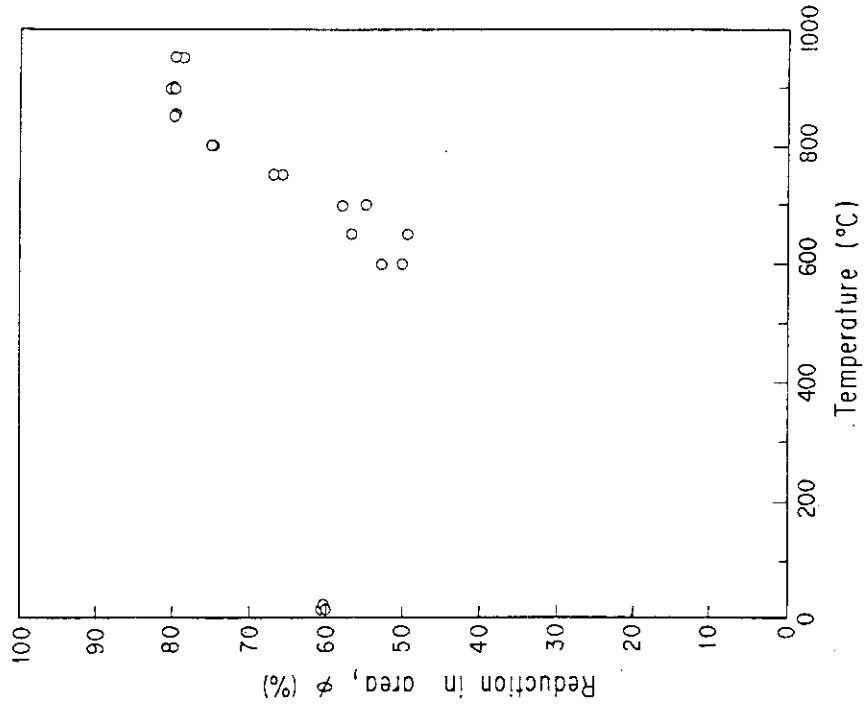

Fig. 5 Reduction in area vs. temperature

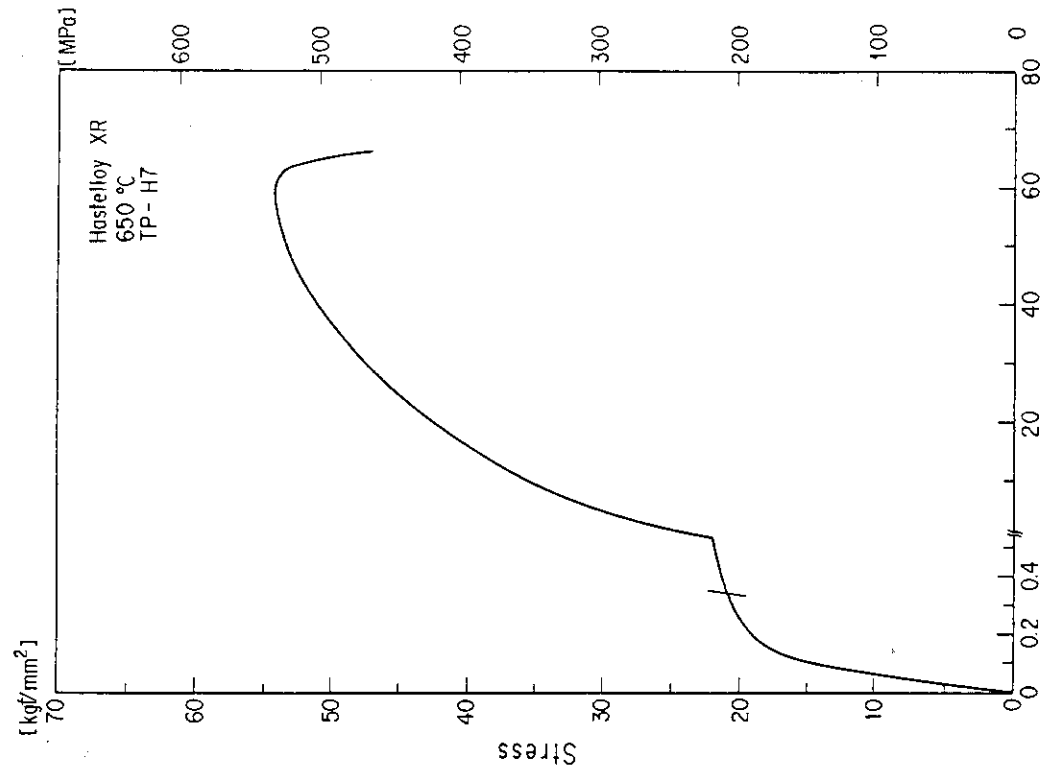

(c) Tested at 650°C

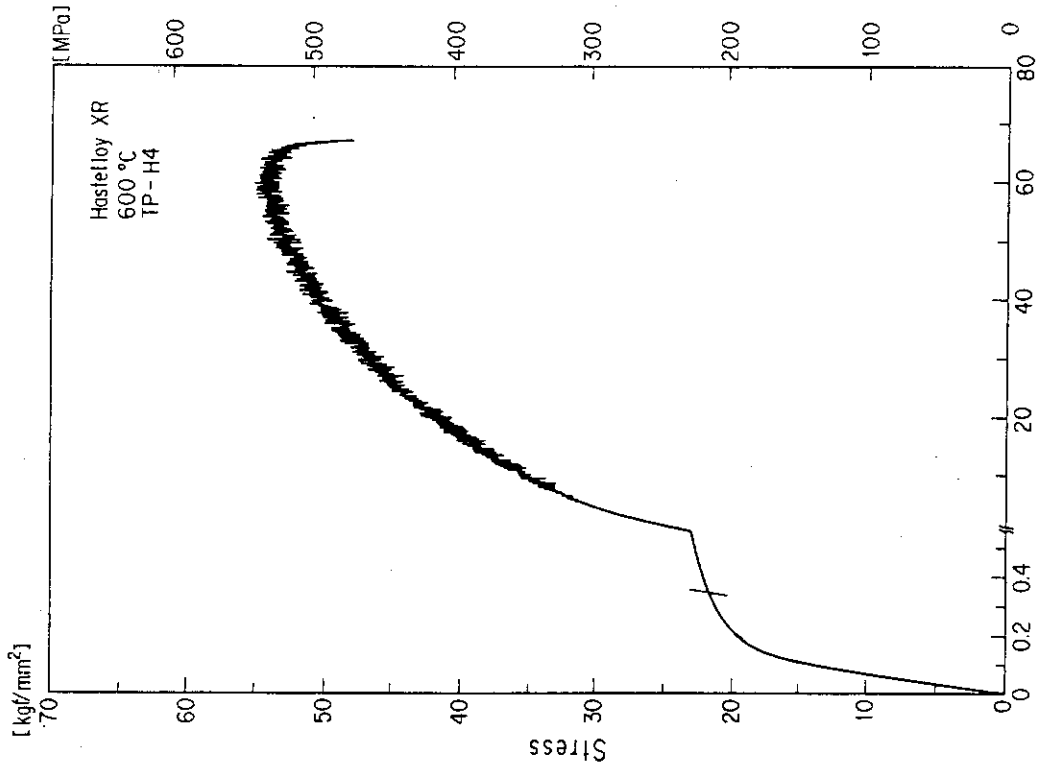

(b) Tested at 600°C

Fig. 6 Tensile stress-strain curves of Hastelloy XR

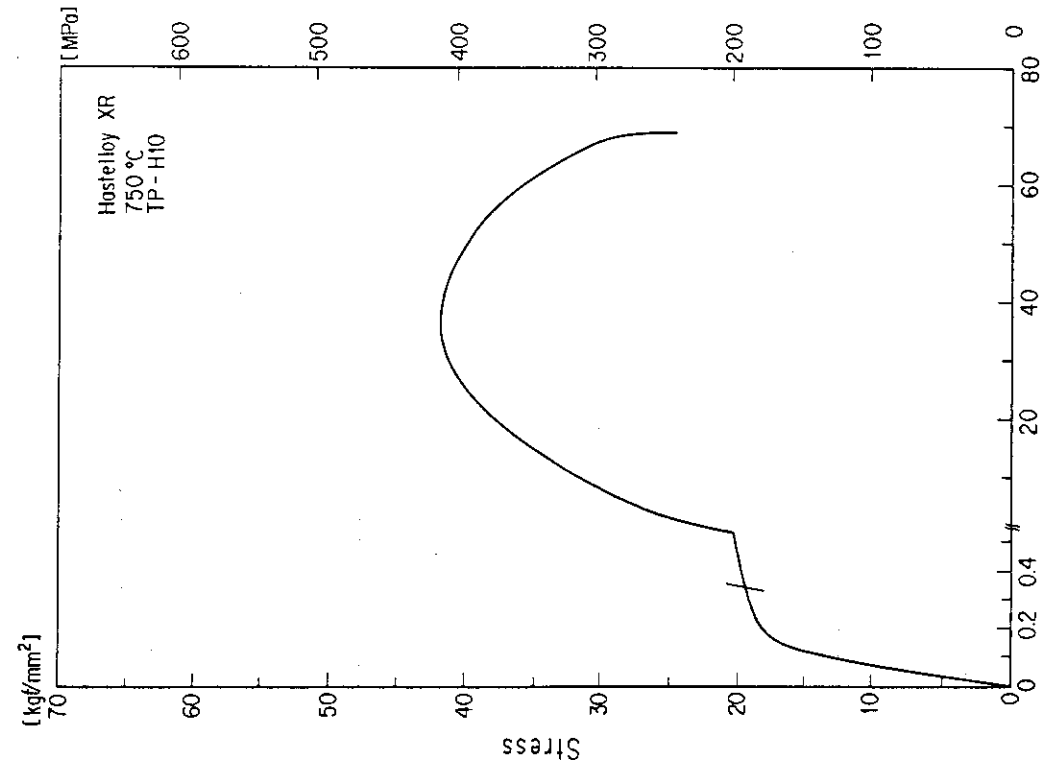

(e) Tested at 750°C

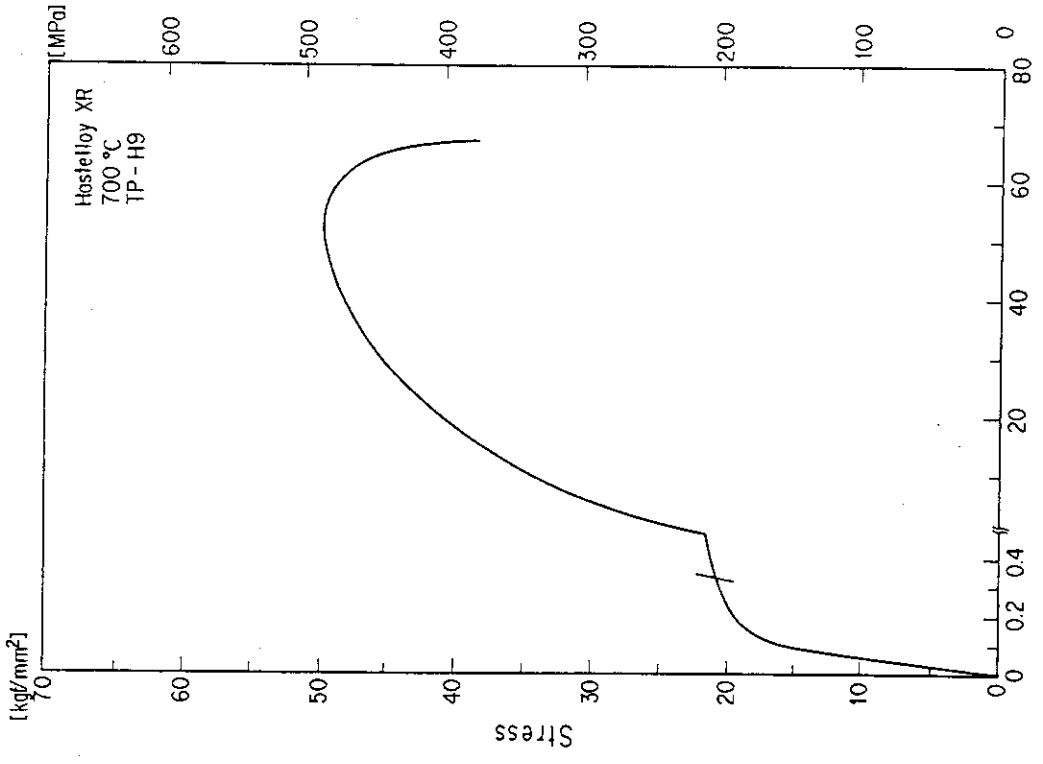

(d) Tested at 700°C

Fig. 6 Tensile stress-strain curves of Hastelloy XR

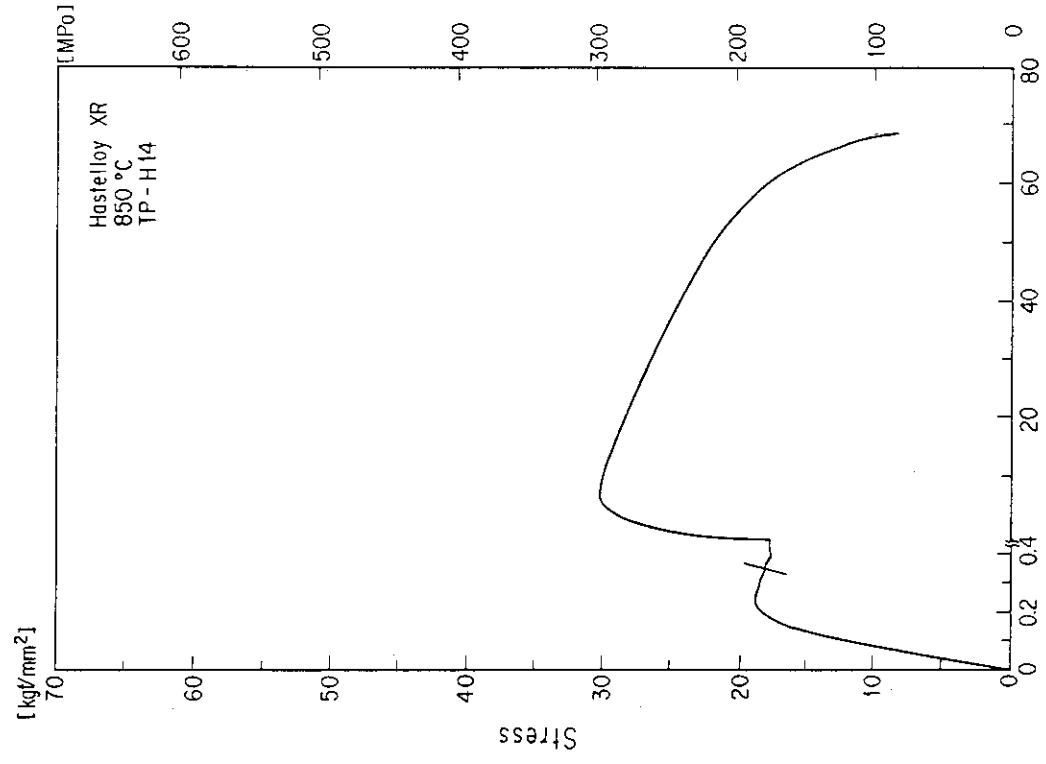

(g) Tested at 850°C

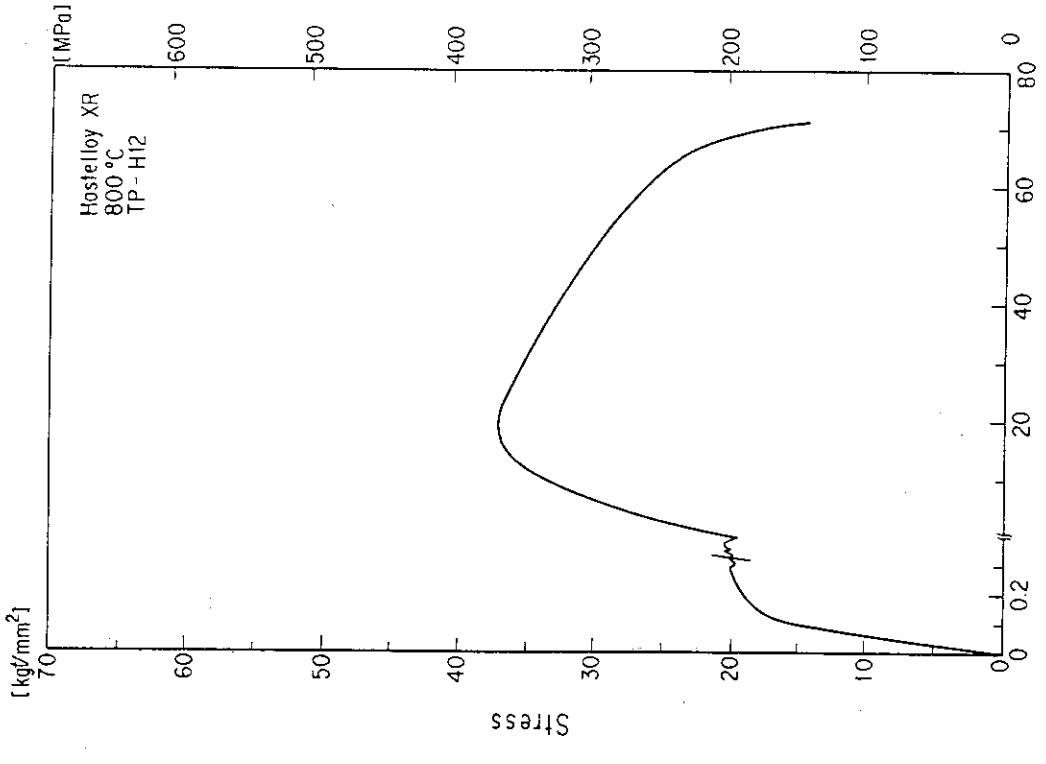

(f) Tested at 800°C

Fig. 6 Tensile stress-strain curves of Hastelloy XR

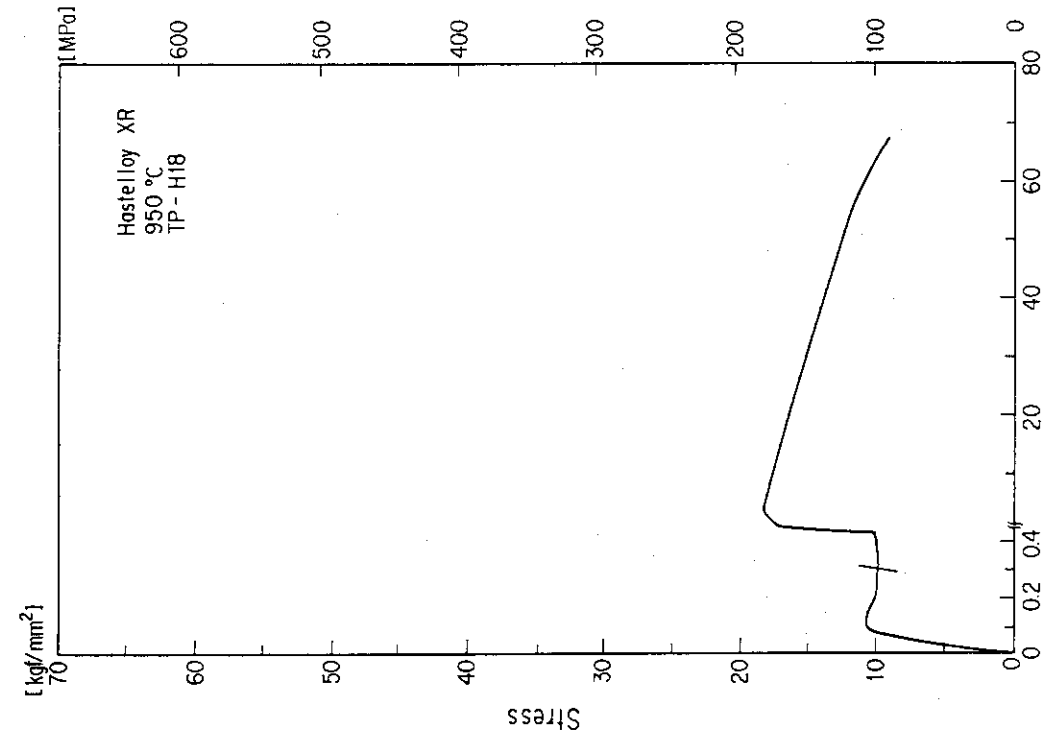

(i) Tested at 950°C

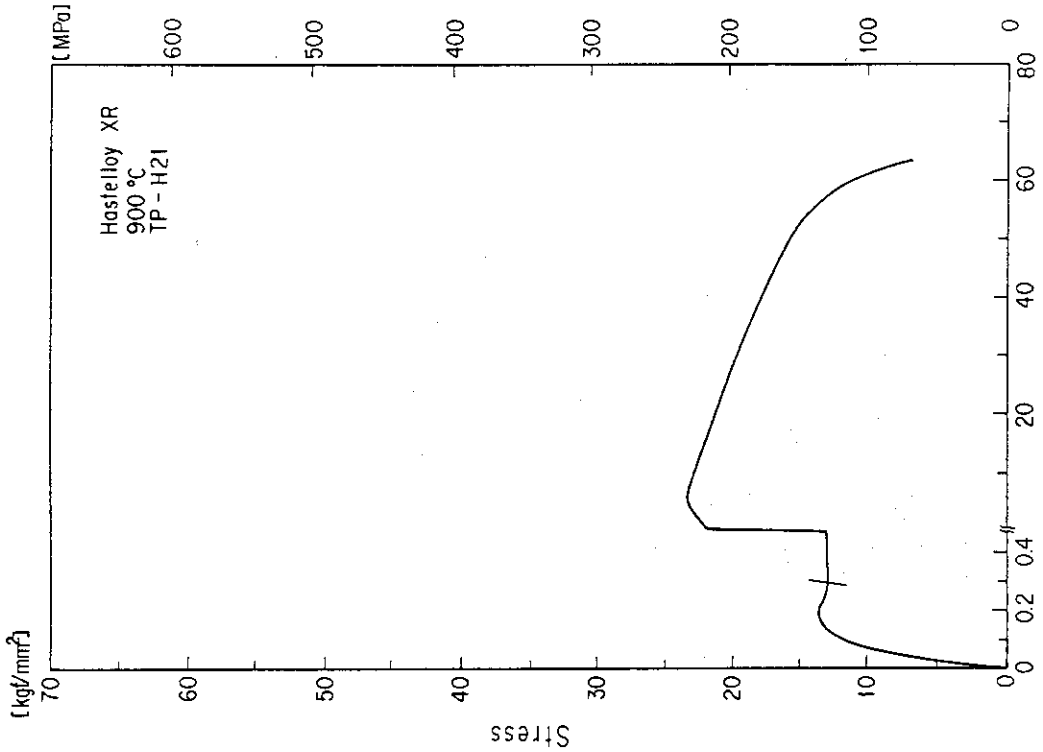

(h) Tested at 900°C

Fig. 6 Tensile stress-strain curves of Hastelloy XR

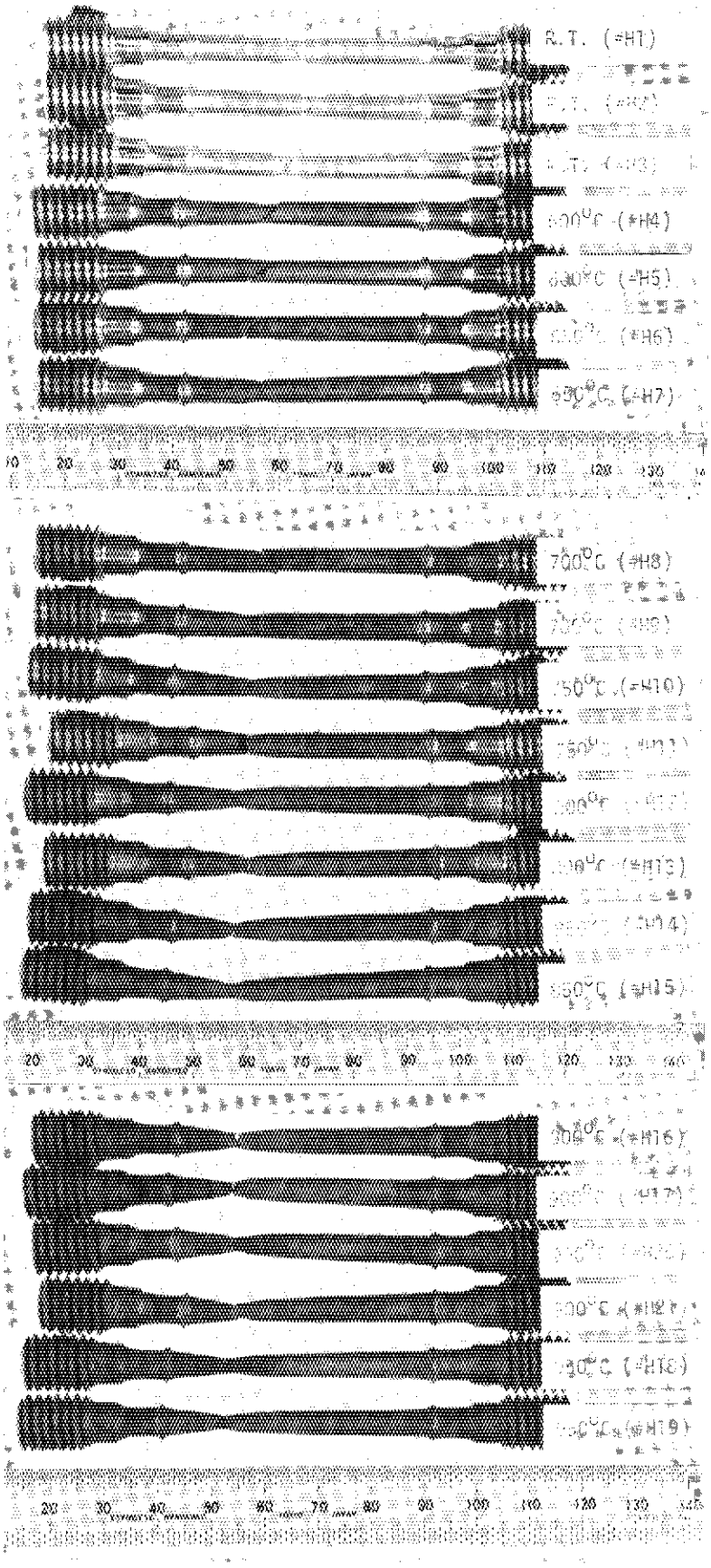

Fig. 7 Appearance of tensile specimens tested

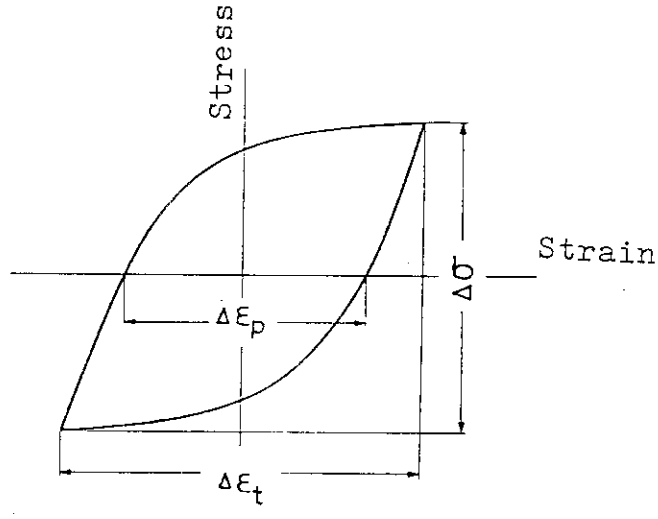

$\Delta\sigma$: Stress range
$\Delta\varepsilon_t$: Total Strain range
$\Delta\varepsilon_p$: Plastic Strain range
$\Delta\varepsilon_e$: Elastic Strain range = $\Delta\varepsilon_t - \Delta\varepsilon_p$

Fig. 8 Schematic hysteresis loop and definitions of parameters

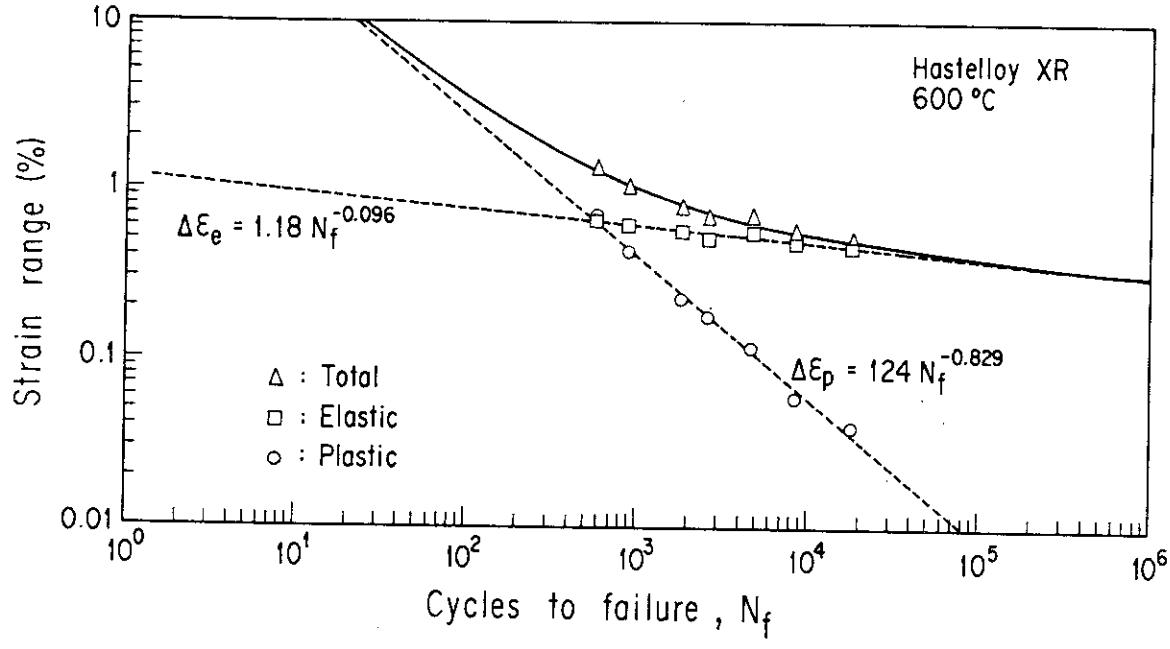

(a) Tested at 600°C

Fig. 9 Fatigue life of Hastelloy XR

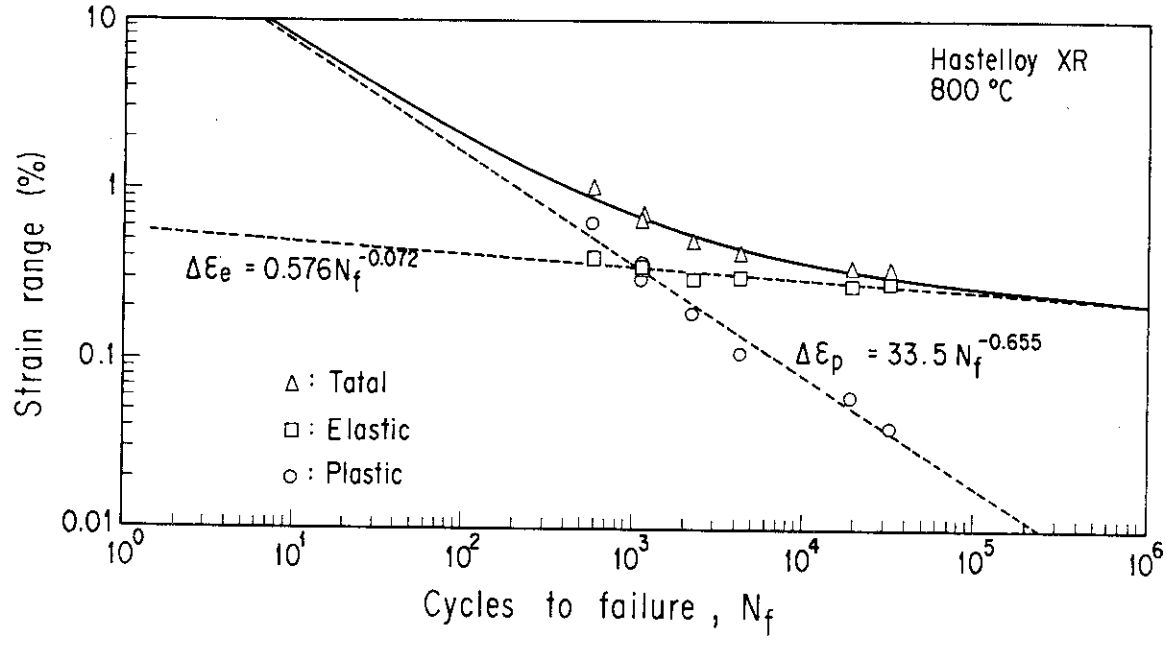

(b) Tested at 800°C

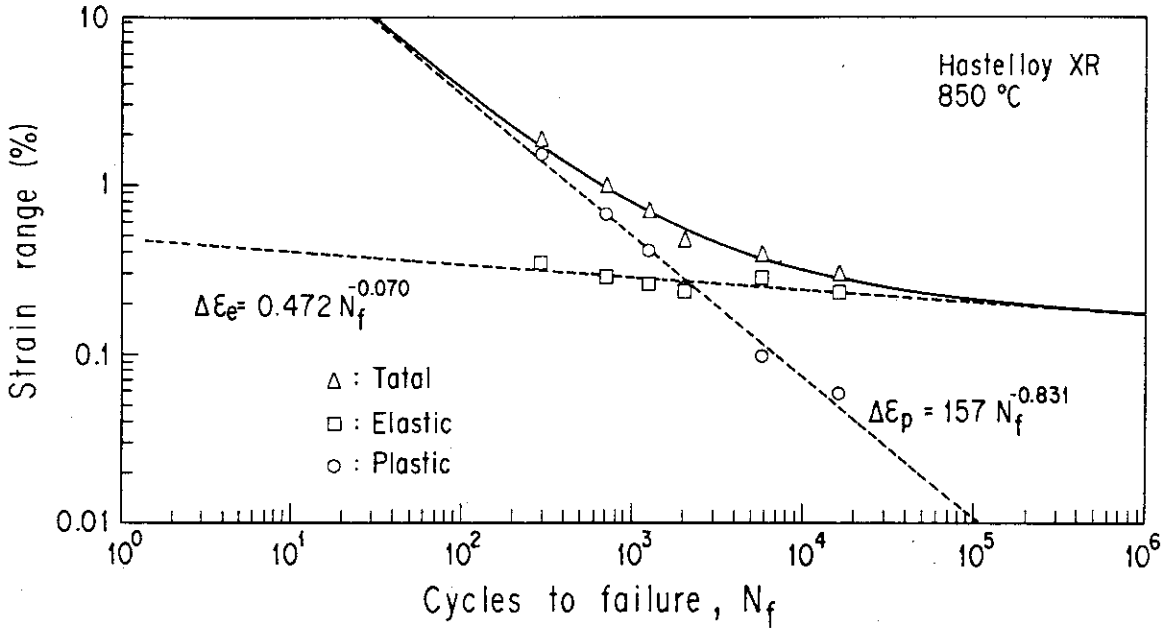

(c) Tested at 850°C

Fig. 9 Fatigue life of Hastelloy XR

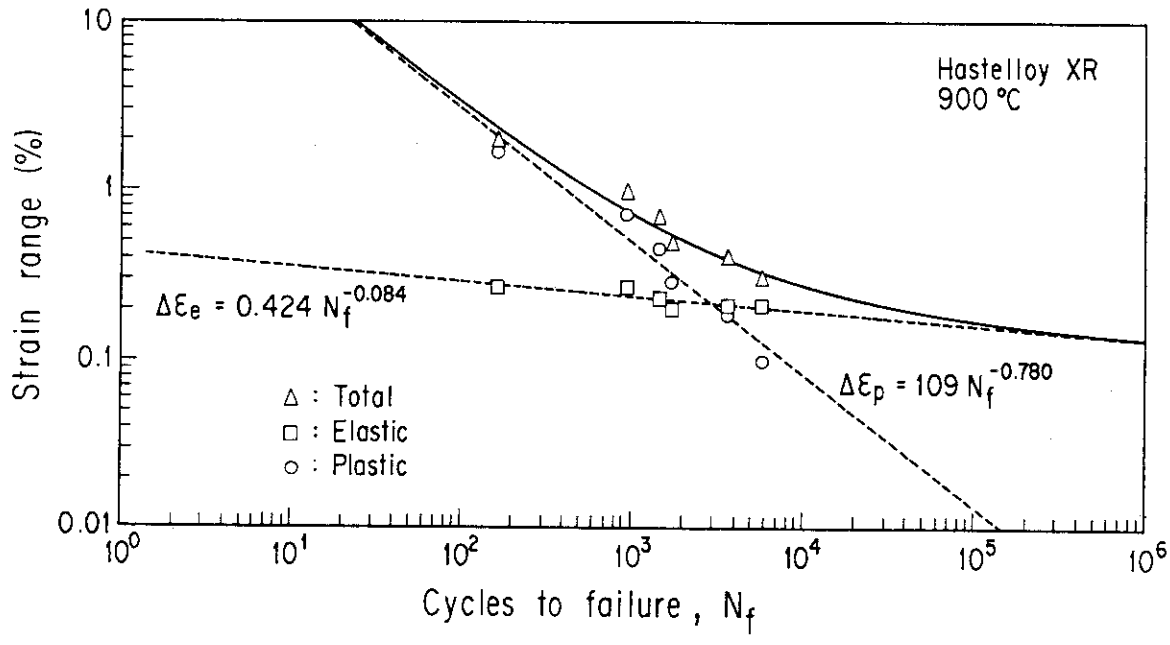

(d) Tested at 900°C

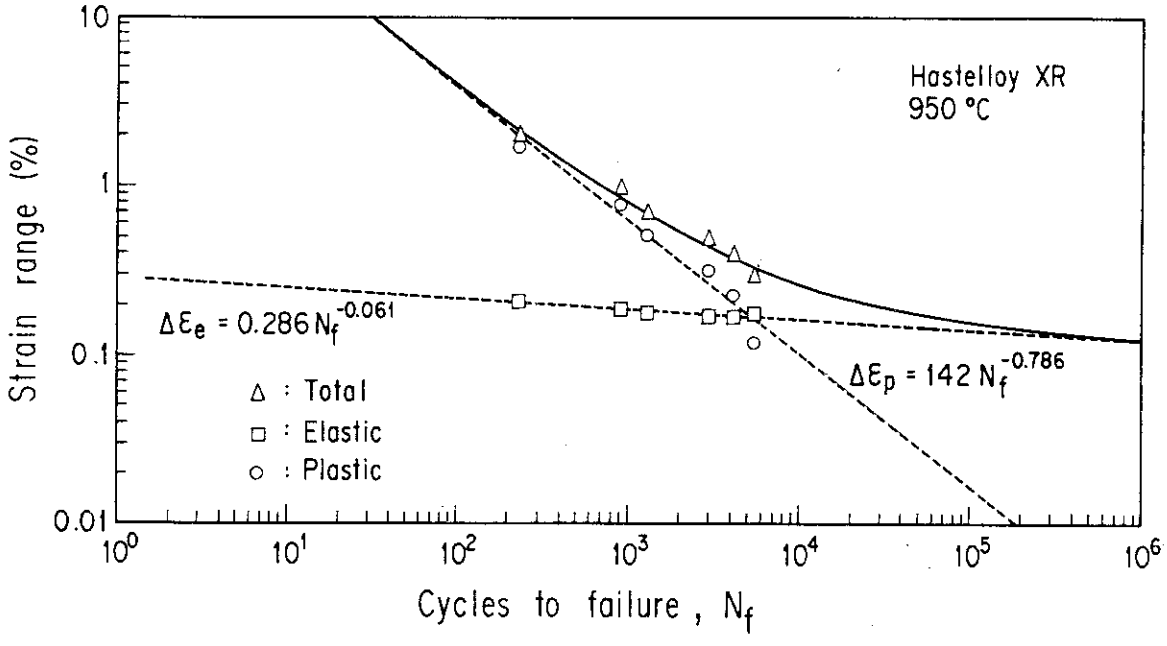

(e) Tseted at 950°C

Fig. 9 Fatigue life of Hastelloy XR

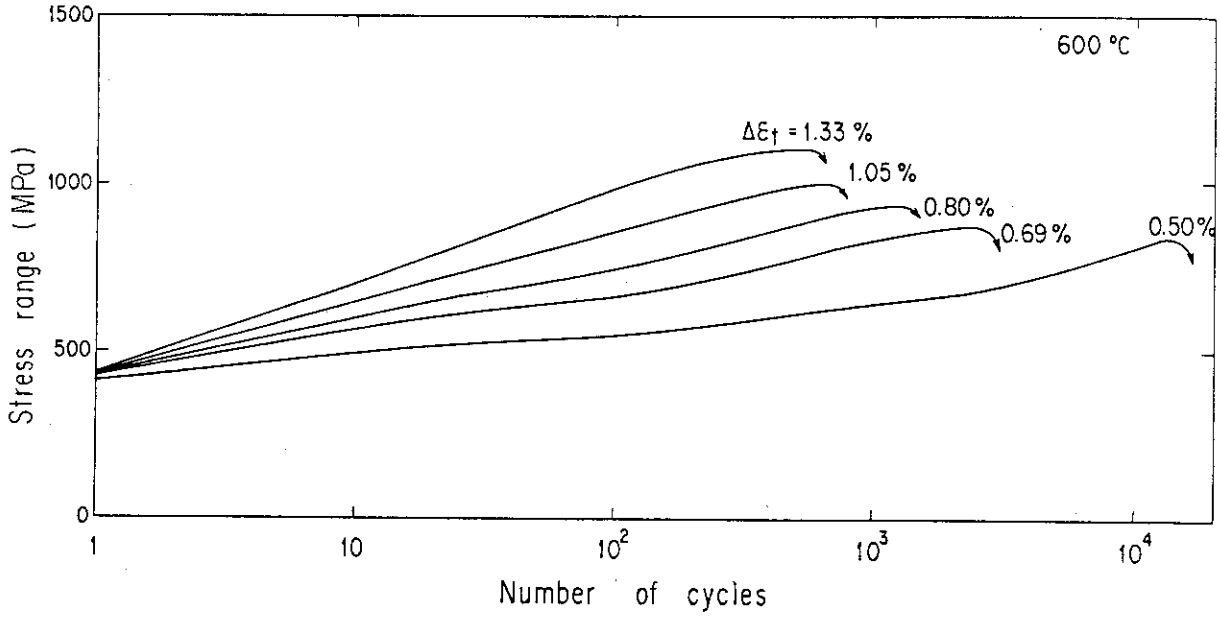

(a) Tested at 600°C

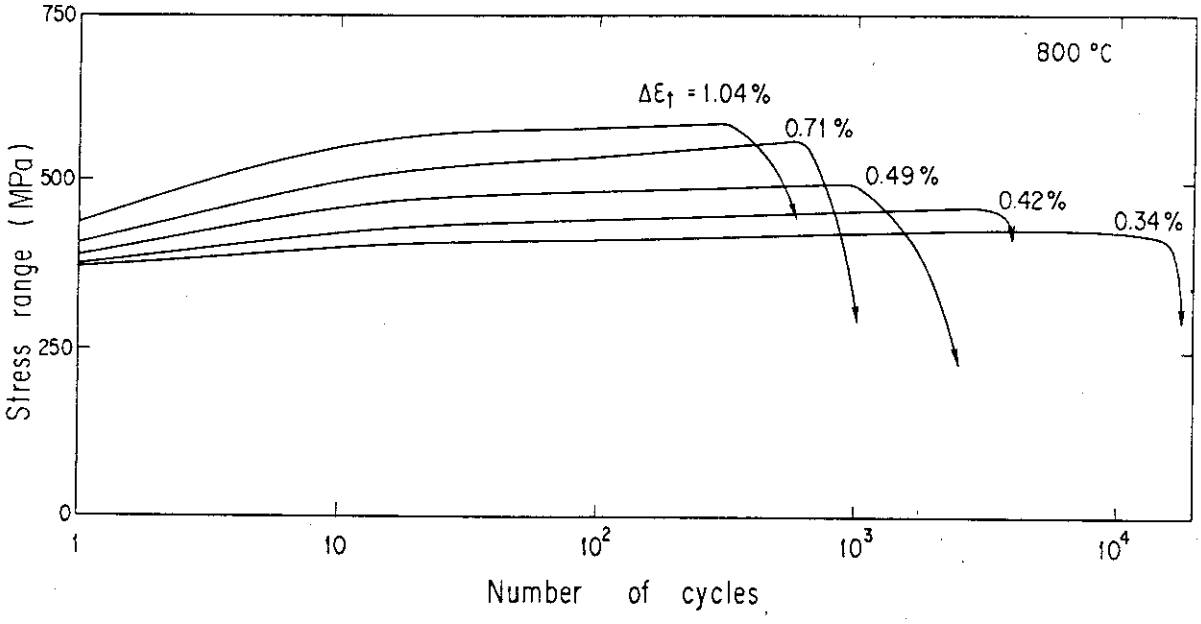

(b) Tested at 800°C

Fig. 10 Change in stress range during cyclic straining

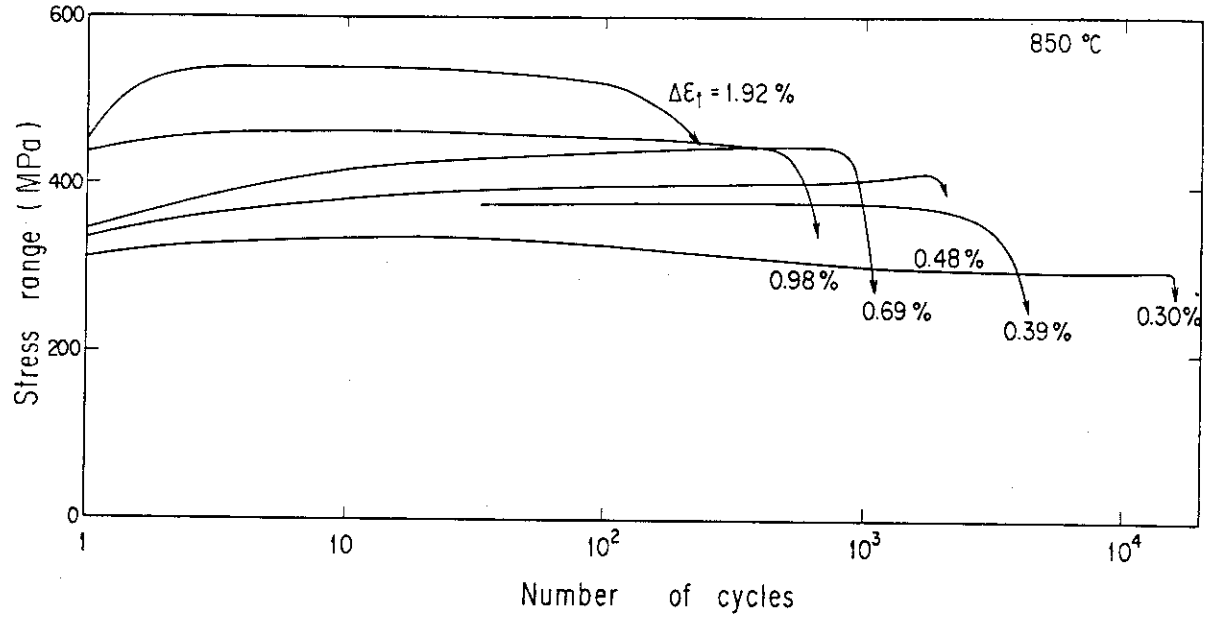

(c) Tested at 850°C

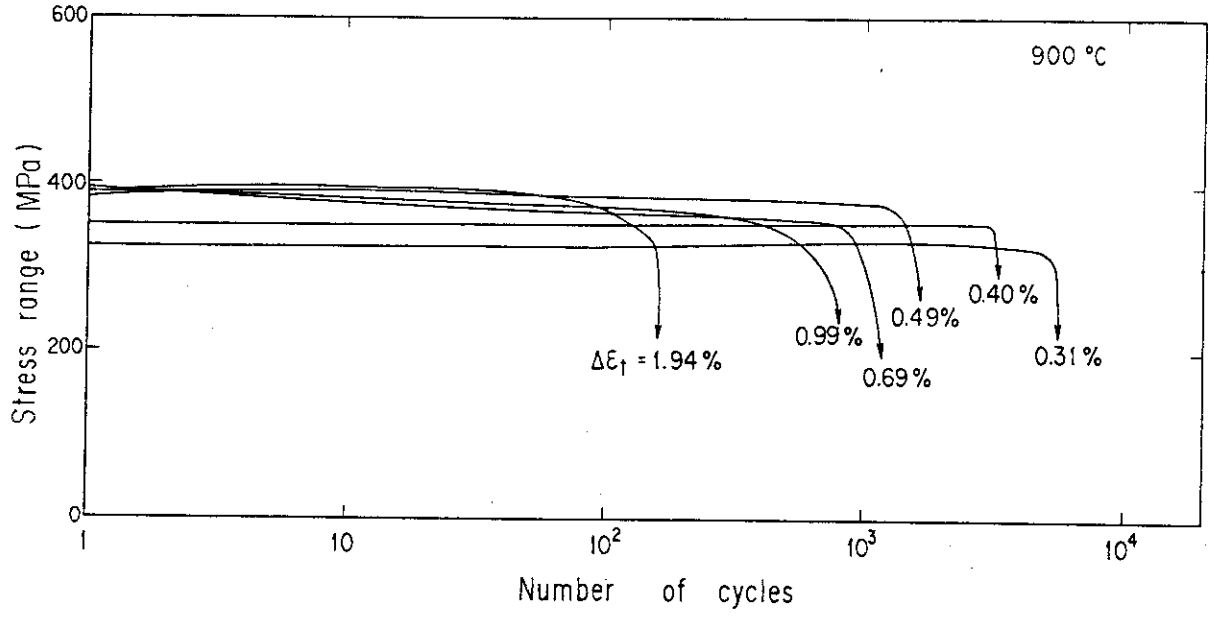

(d) Tested at 900°C

Fig. 10 Change in stress range during cyclic straining

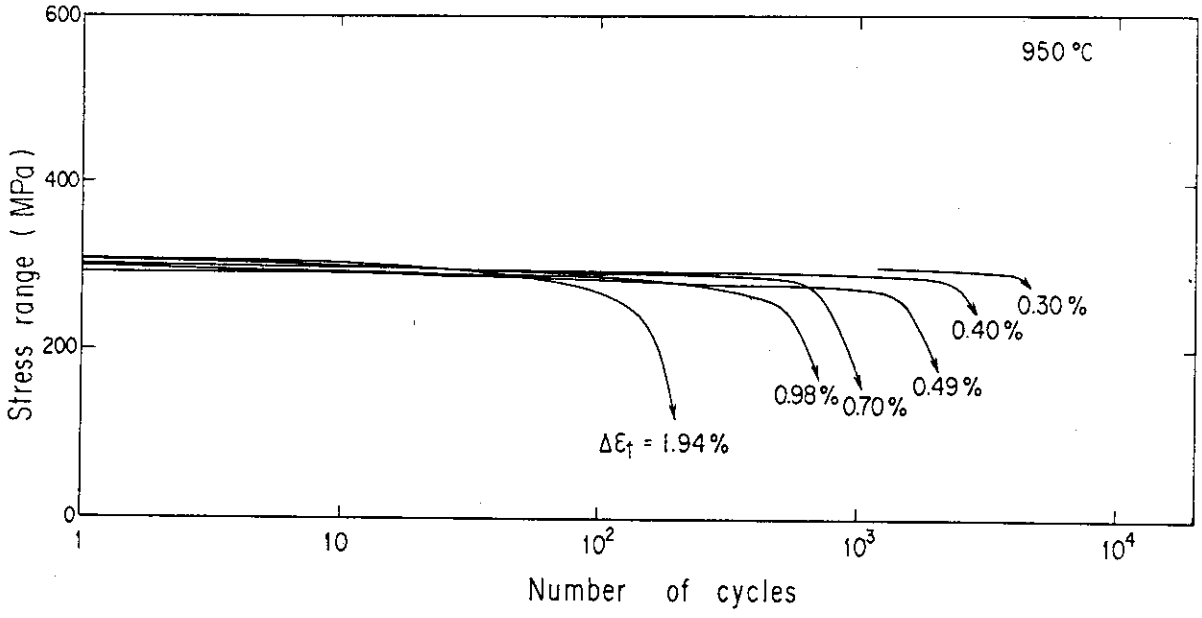

(e) Tested at 950°C

Fig. 10 Change in stress range during cyclic straining

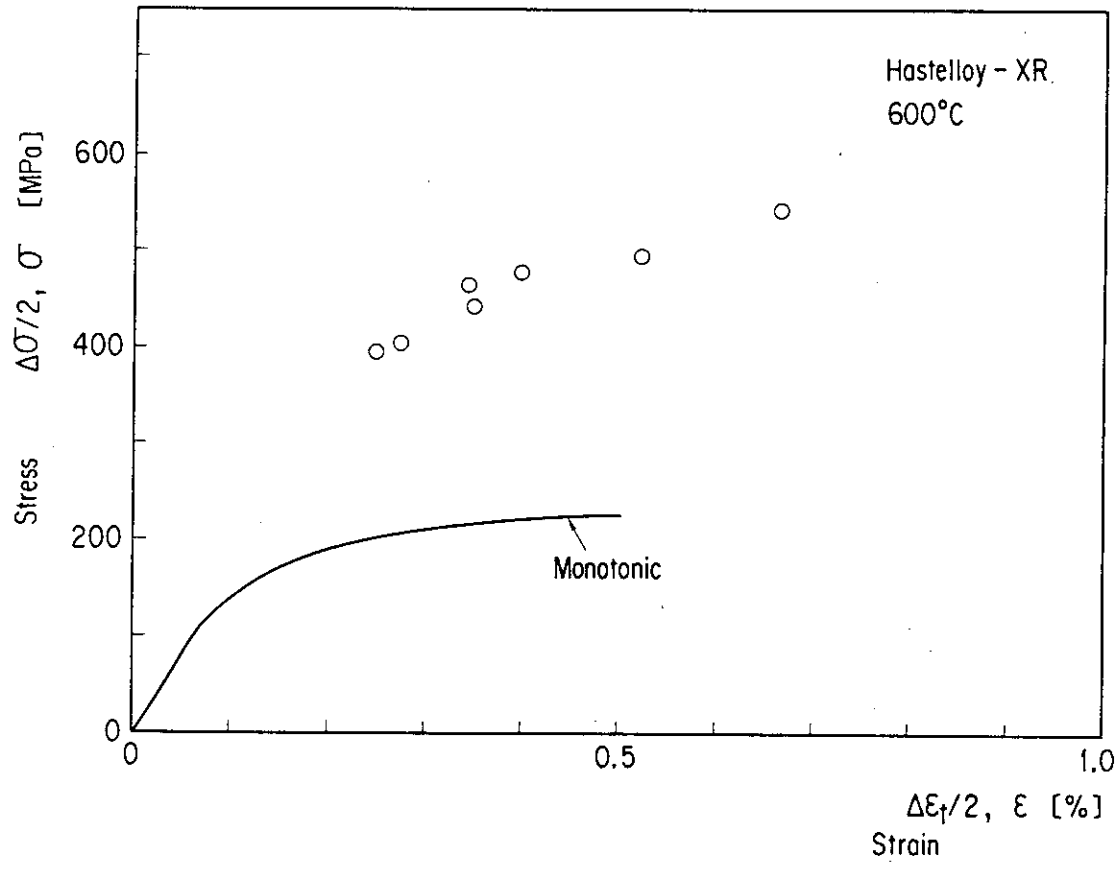

(a) Tested at 600°C

Fig. 11 Cyclic stress-strain curves of Hastelloy XR

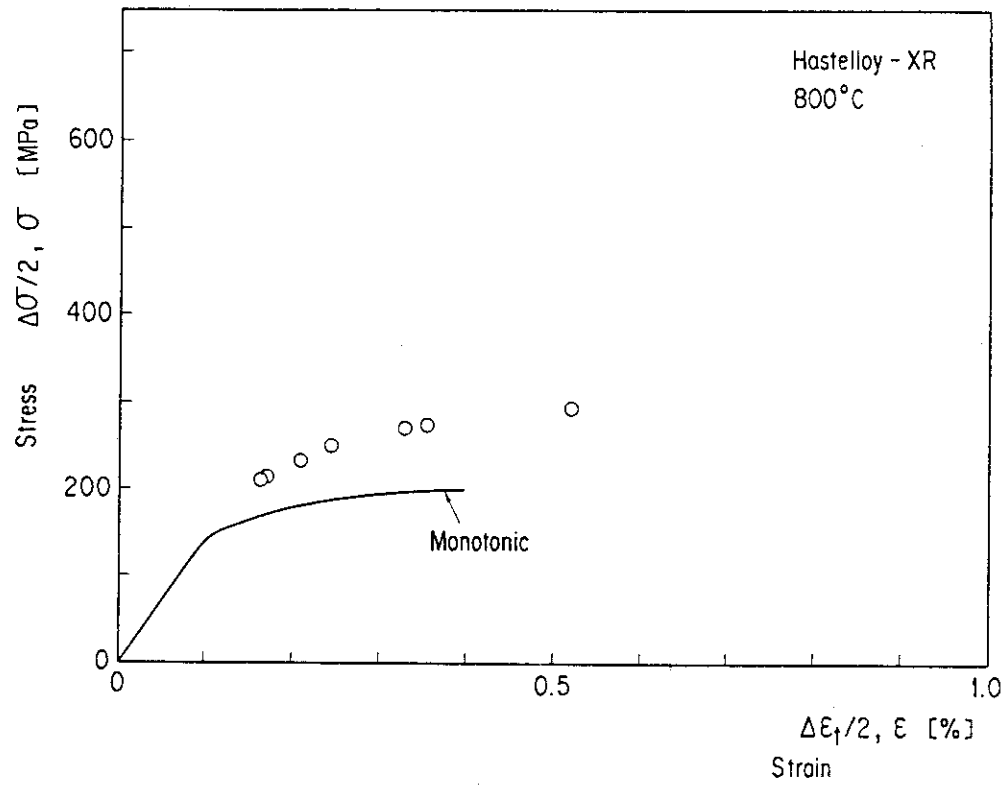

(b) Tested at 800°C

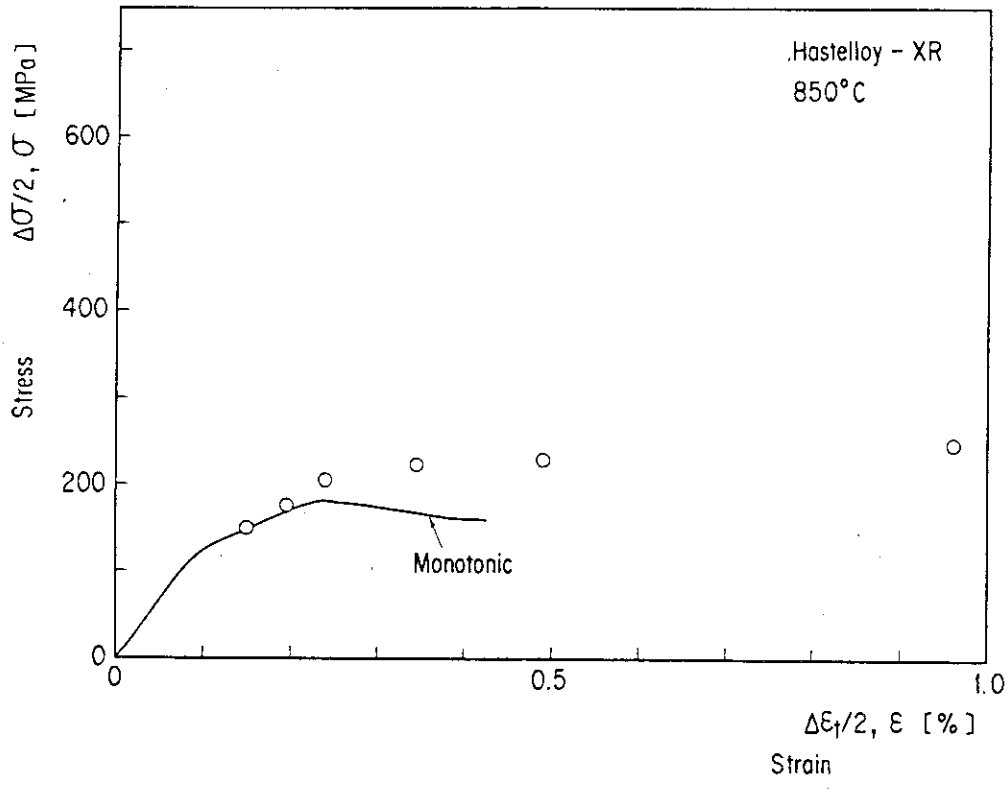

(c) Tested at 850°C

Fig. 11 Cyclic stress-strain curves of Hastelloy XR

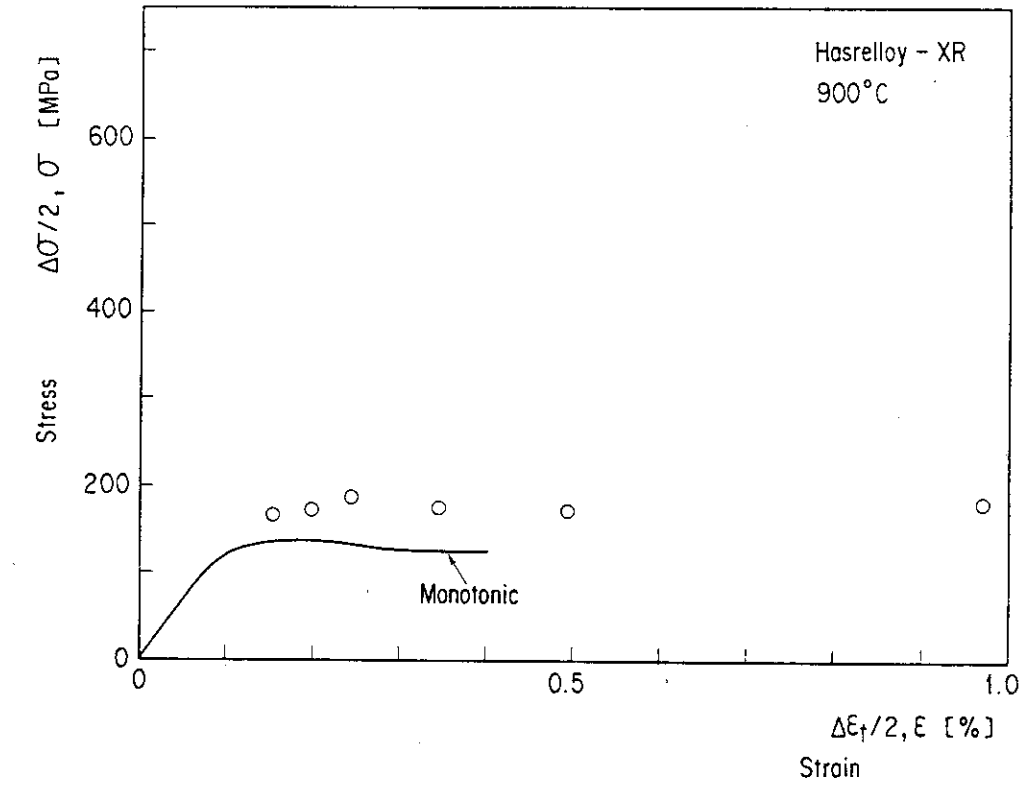

(d) Tested at 900°C

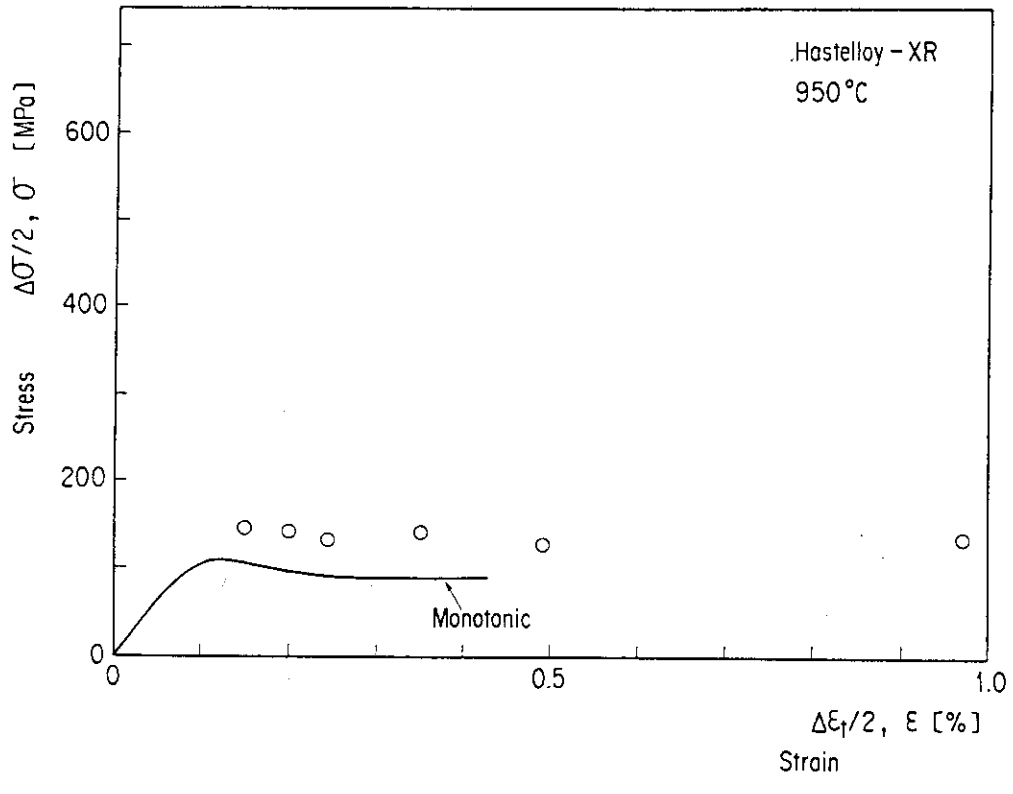

(e) Tested at 950°C

Fig. 11 Cyclic stress-strain curves of Hastelloy XR

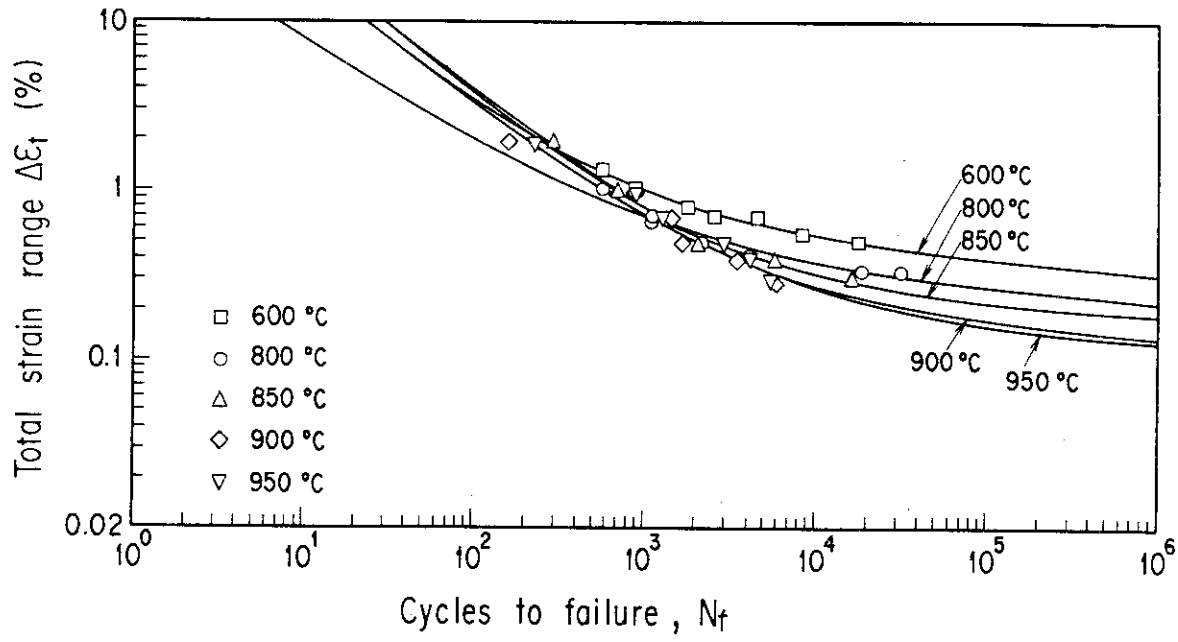

Fig. 12 Temperature dependence of $\Delta\varepsilon_t$-Nf curves

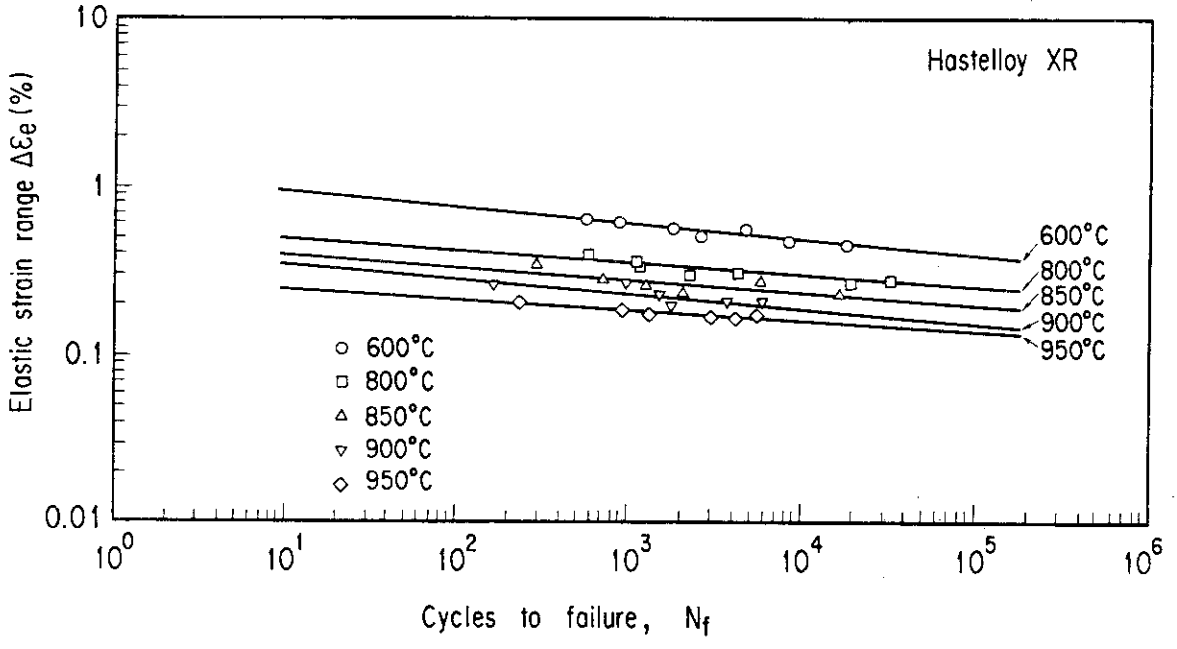

Fig. 13 Temperature dependence of $\Delta\varepsilon_e$-Nf relationship

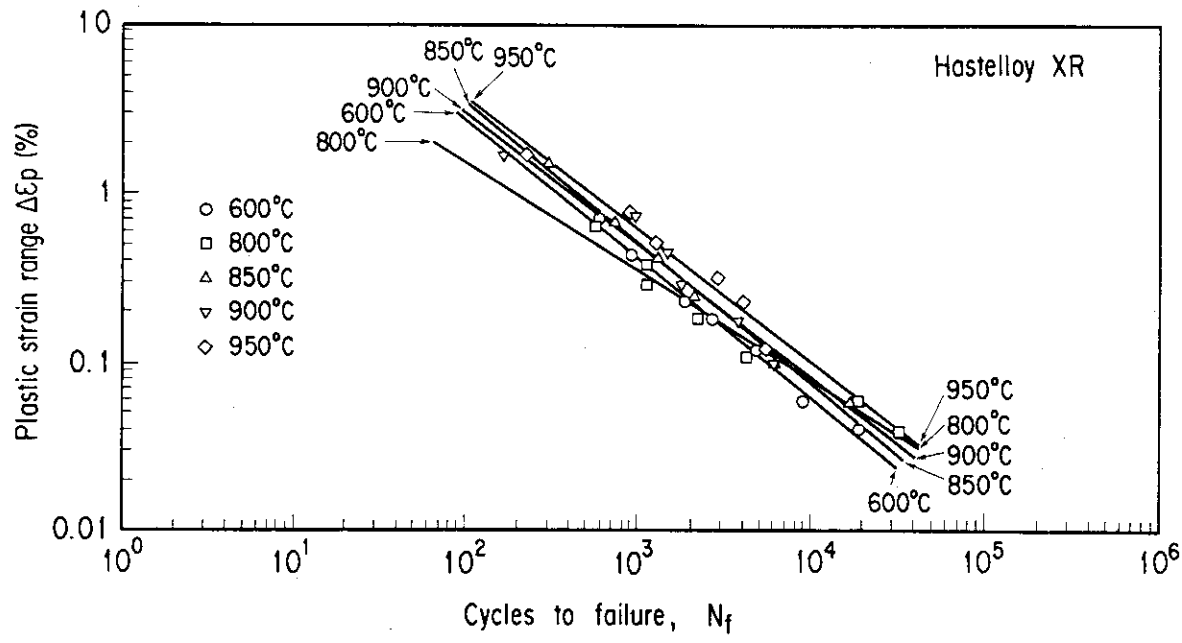

Fig. 14 Temperature dependence of $\Delta\varepsilon_p$-Nf relationship

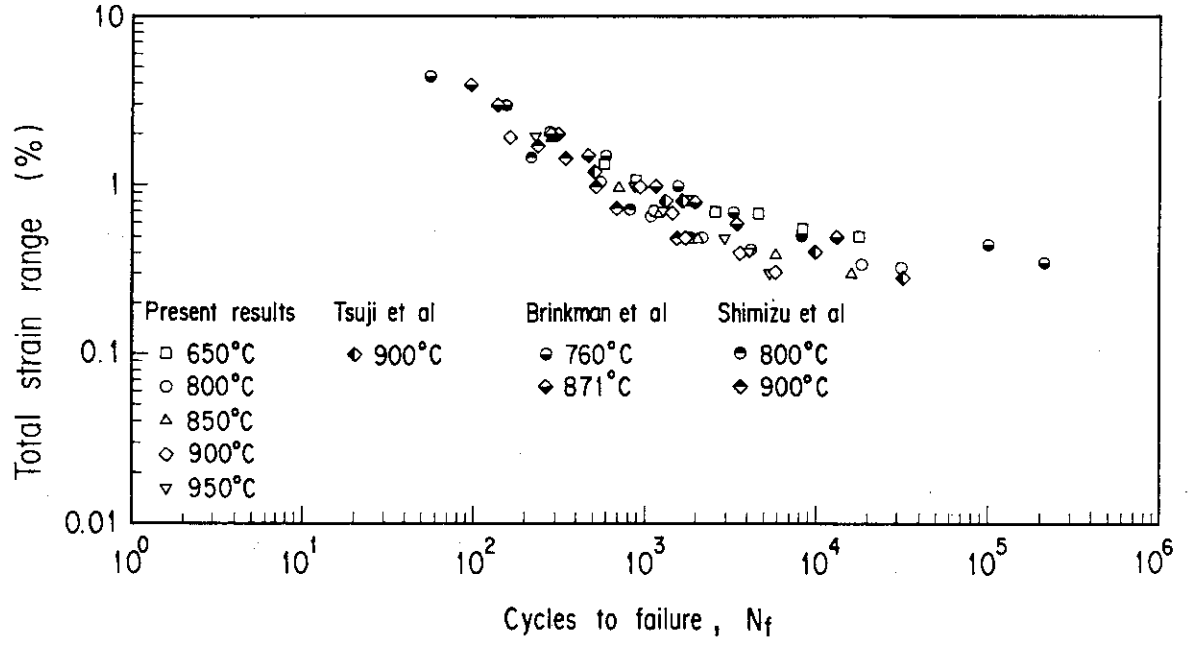

Fig. 15 Fatigue data of Hastelloy XR and Hastelloy X from references with present data

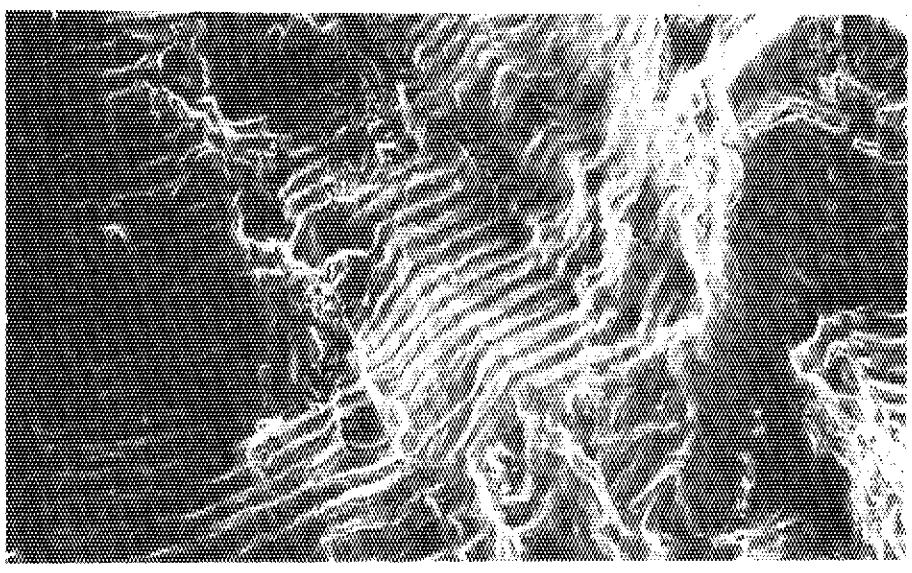

(a) 600°C, $\Delta\varepsilon_t$ = 1.33 %

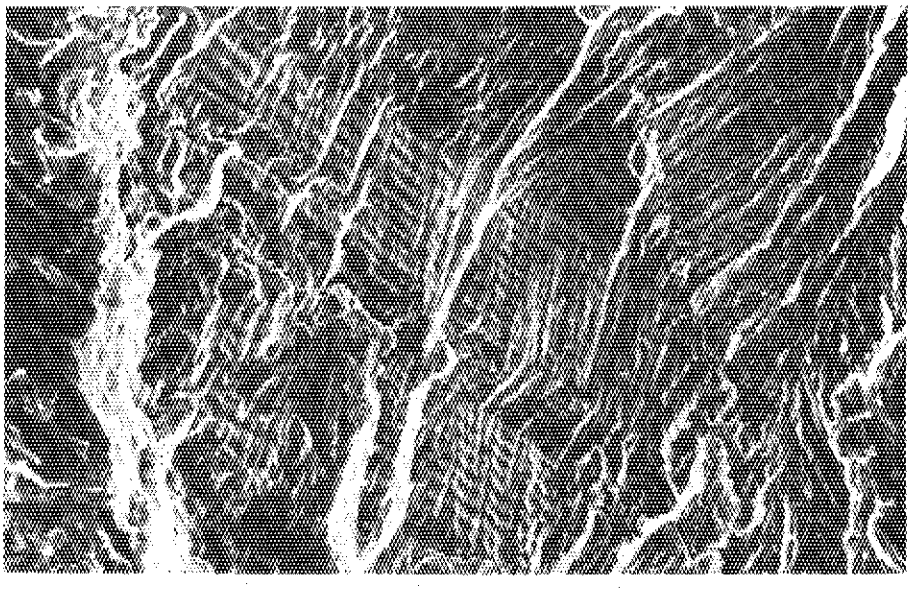

(b) 800°C, $\Delta\varepsilon_t$ = 1.04 %

Fig. 16 Microphotographs of fracture surfaces of fatigued specimens

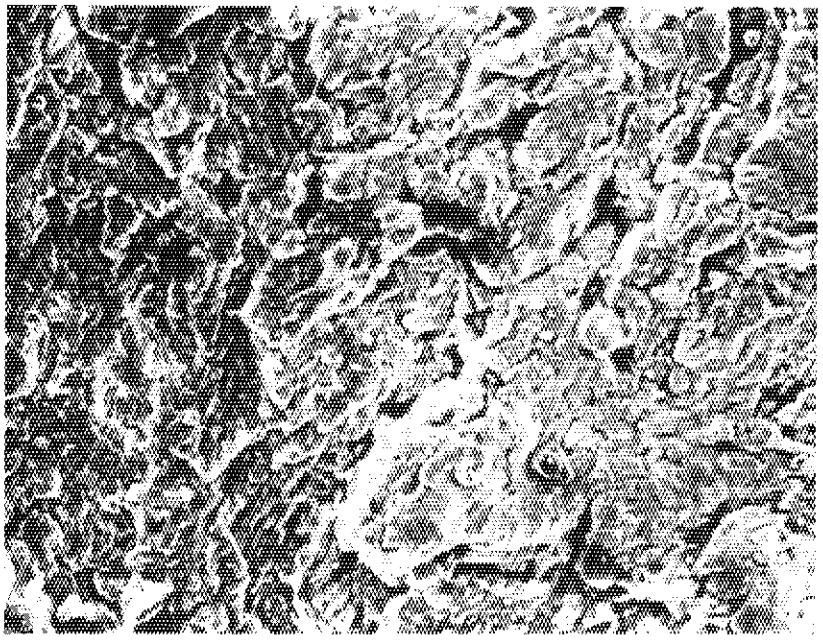

(c) 850°C, $\Delta\varepsilon_t$ = 0.98 %

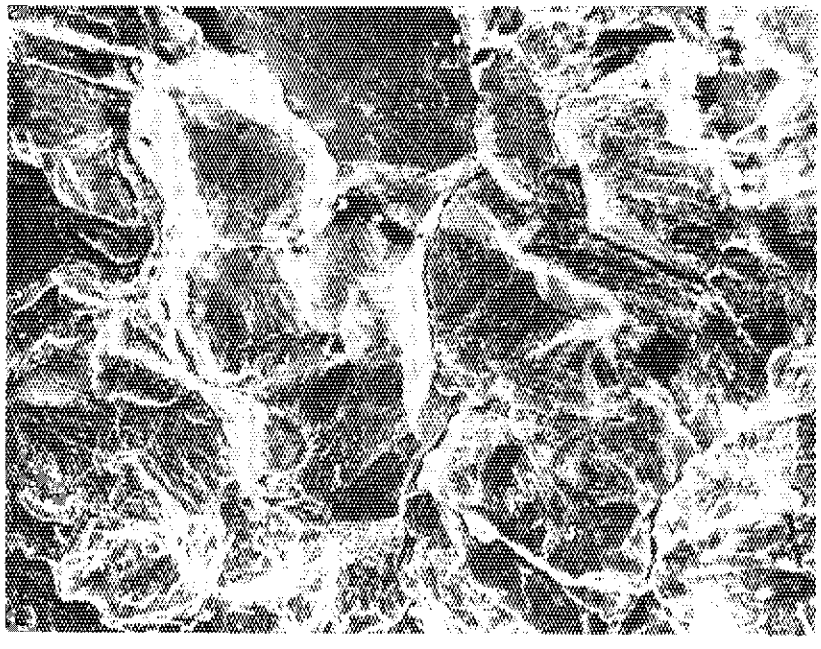

(d) 900°C, $\Delta\varepsilon_t$ = 0.99 %

Fig. 16 Microphotographs of fracture surfaces of fatigued specimens

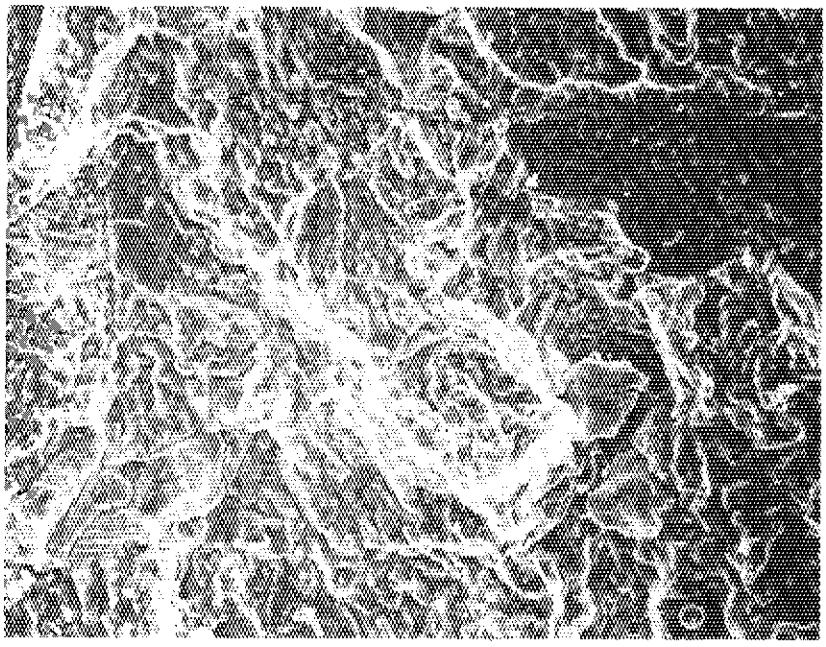

(e) 950°C, $\Delta\varepsilon_t$ = 0.98 %

Fig. 16 Microphotographs of fracture surfaces of fatigued specimens

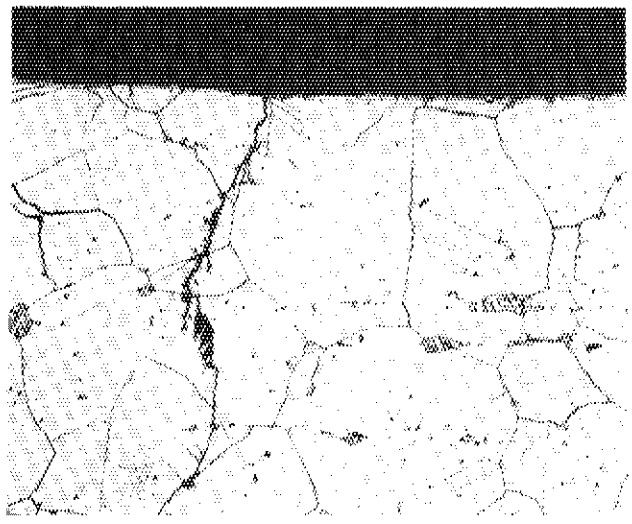

(a) 600°C, $\Delta\varepsilon_t$ = 1.33 %　　100 μm

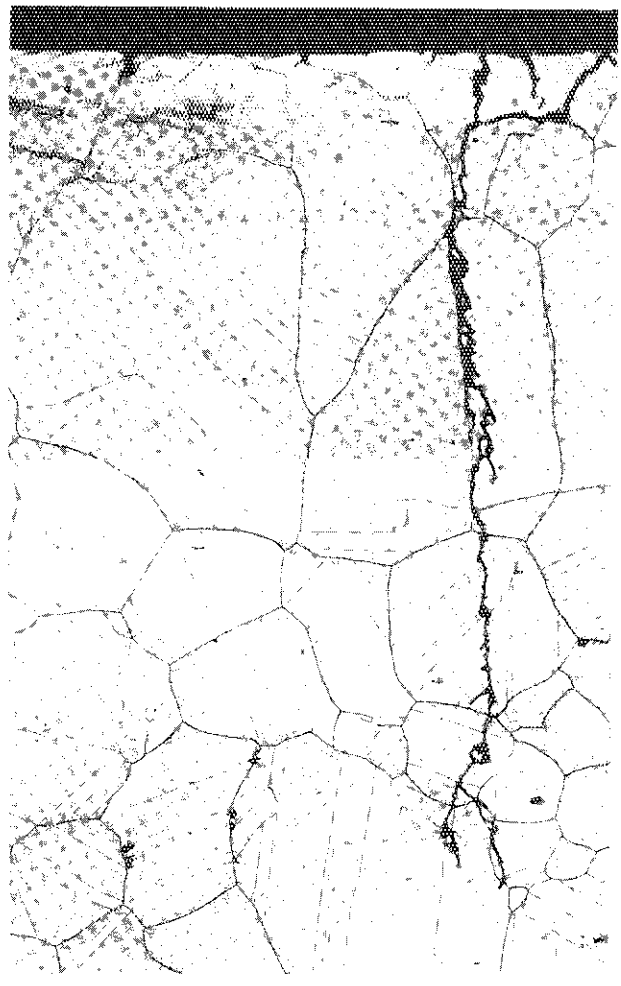

(b) 800°C, $\Delta\varepsilon_t$ = 1.04 %　　100 μm

Fig. 17 Fatigue cracks observed at cross section of fatigued specimens

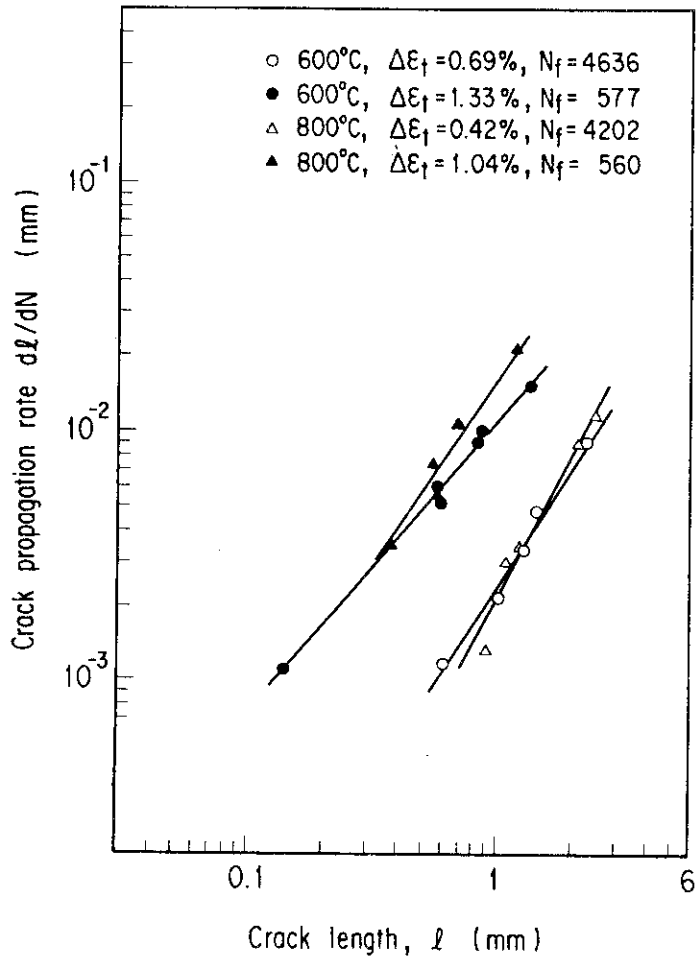

Fig. 18 Relationship between crack propagation rate and crack length

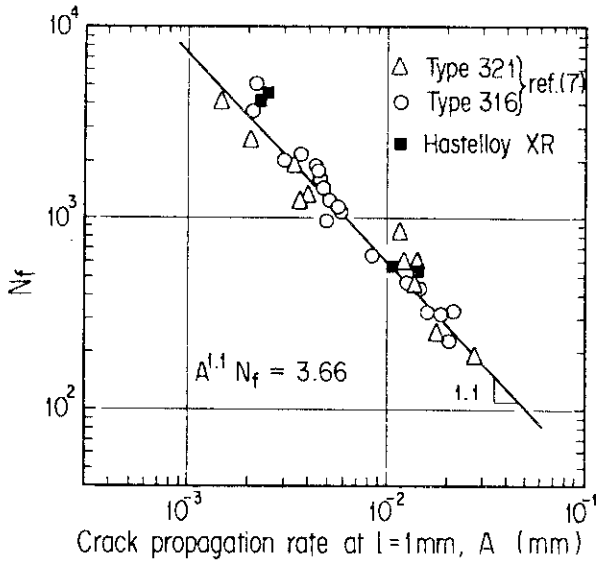

Fig. 19 Relationship between fatigue life and coefficient A in Eq. (4)

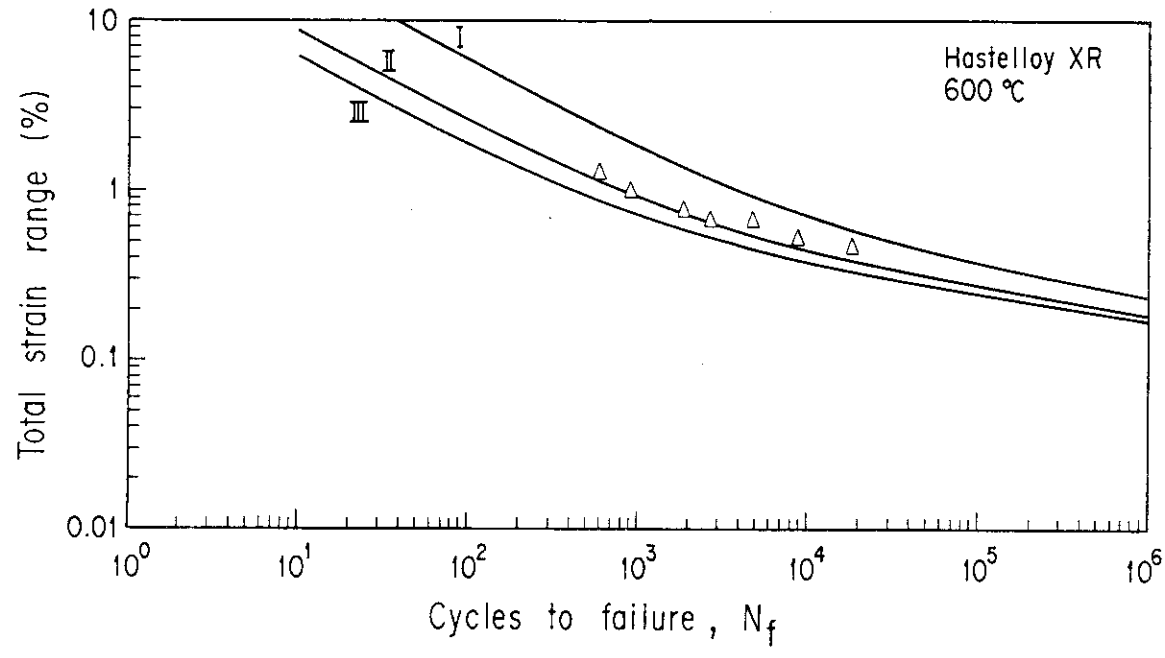

(a) For test temperature of 600°C

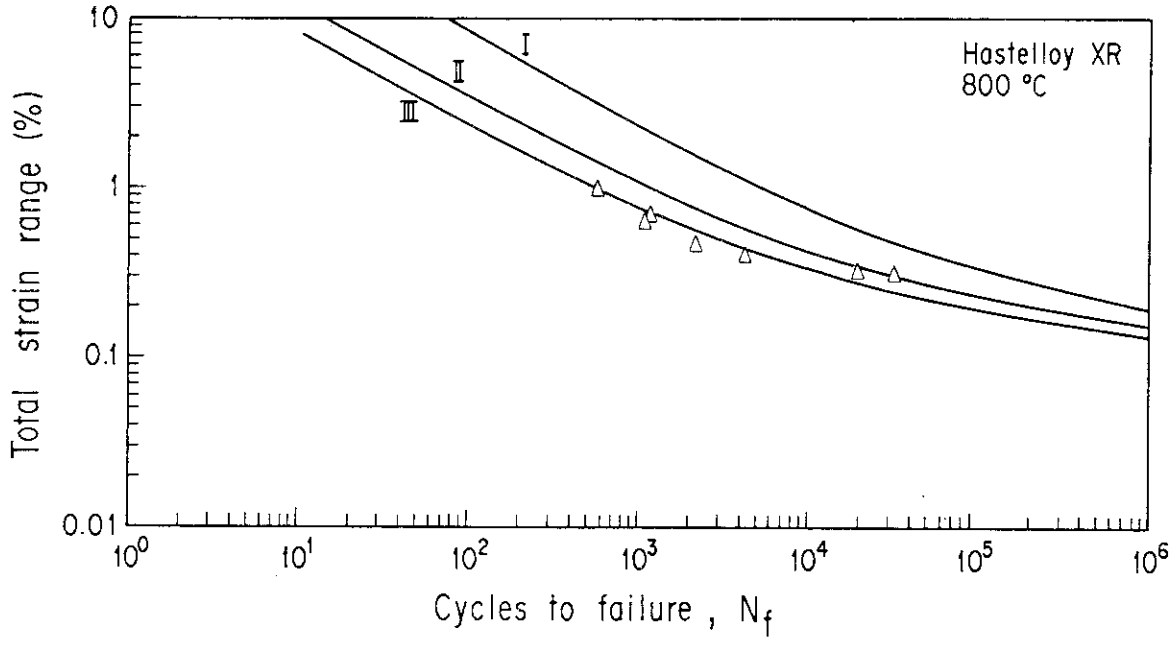

(b) For test temperature of 800°C

Fig. 20 Estimation of fatigue life by Manson's method

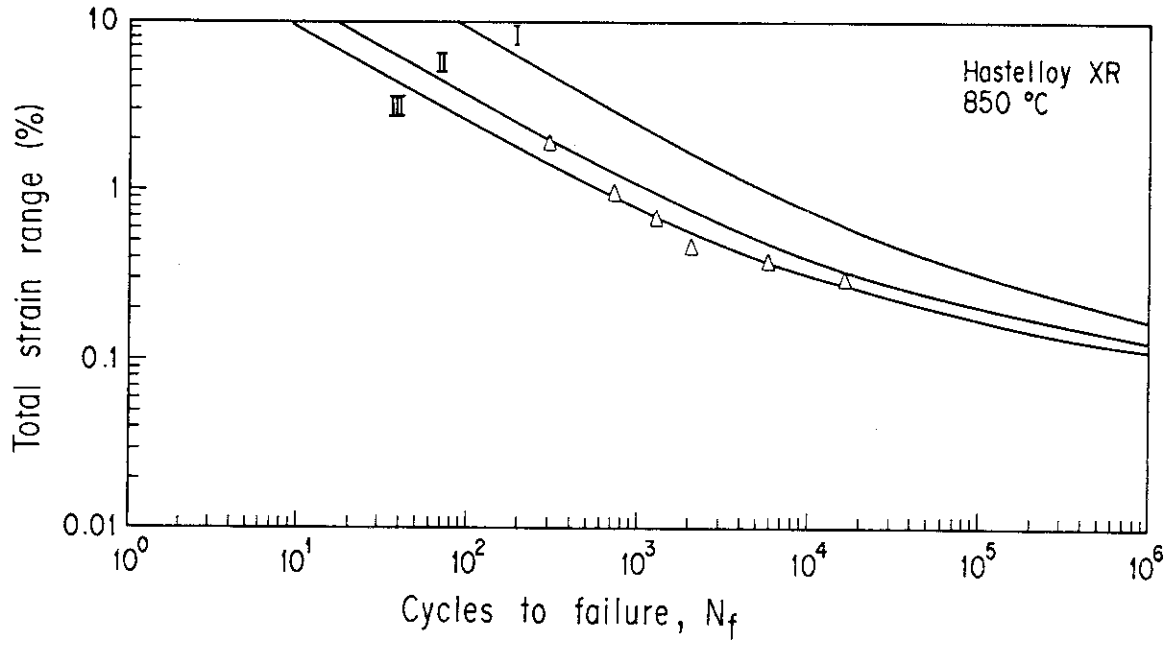

(c) For test temperature of 850°C

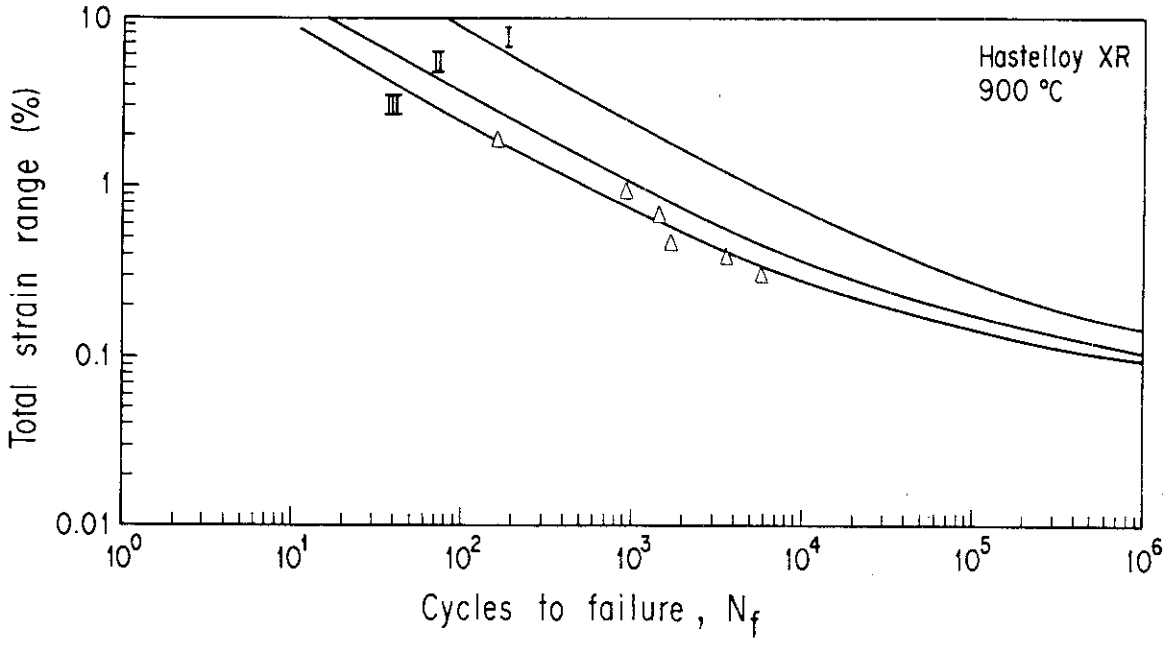

(d) For test temperature of 900°C

Fig. 20 Estimation of fatigue life by Manson's method

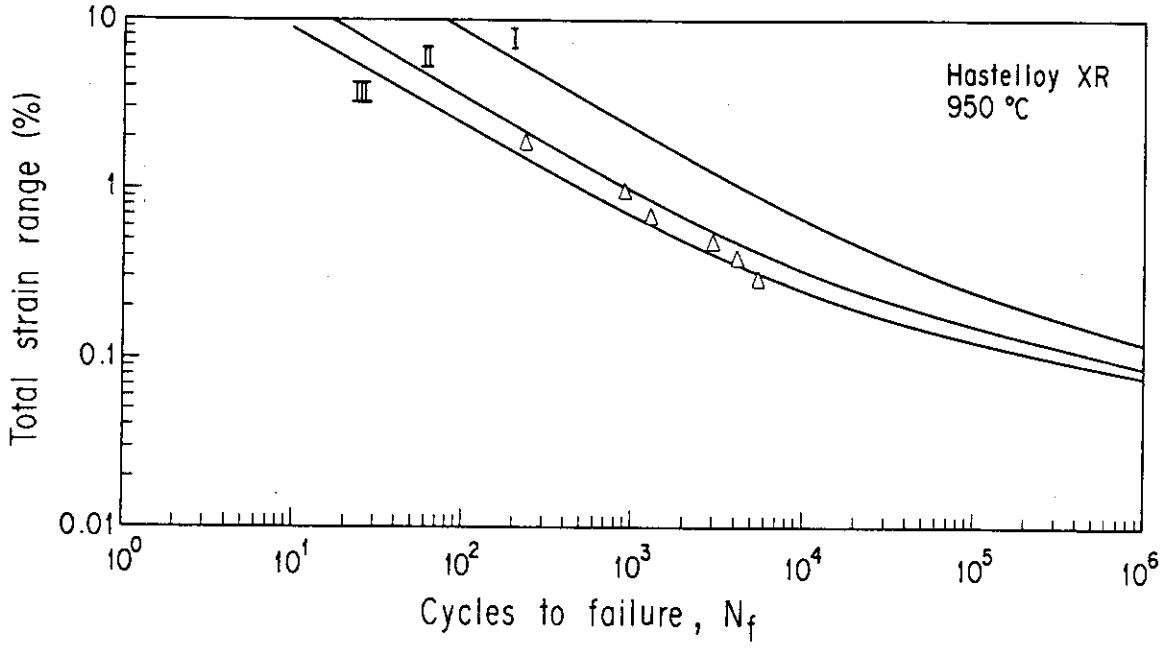

(e) For test temperature of 950°C

Fig. 20 Estimation of fatigue life by Manson's method

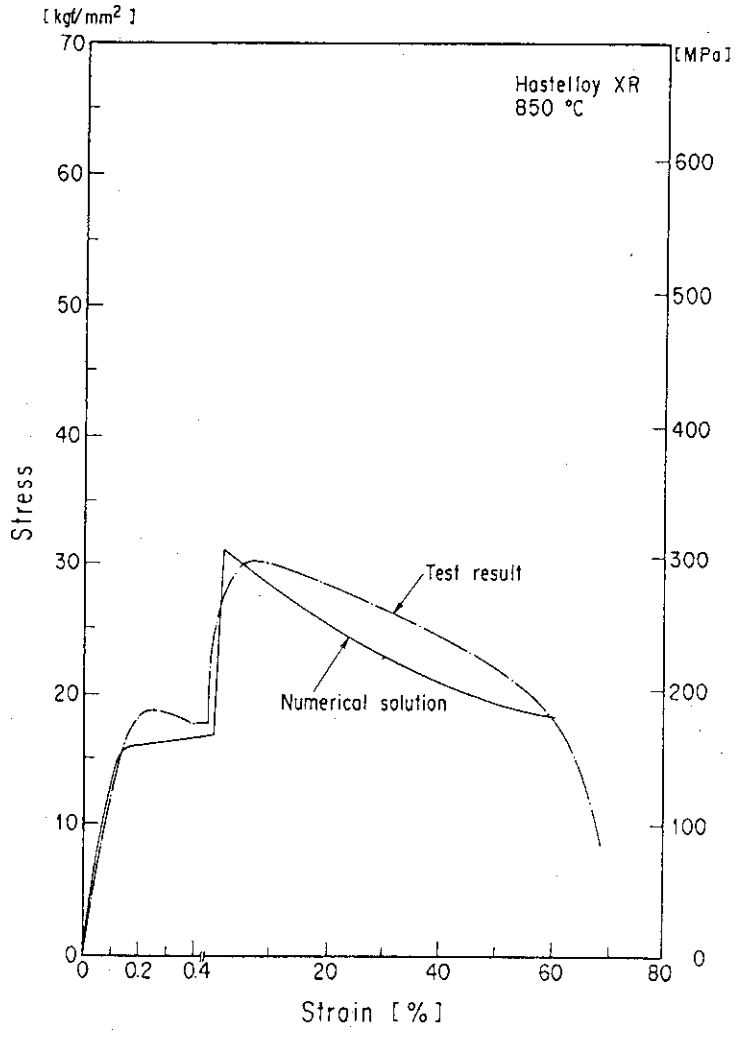

(a) For test temperature of 850°C

Fig. 21 Tensile stress-strain curves obtained by numerical analysis

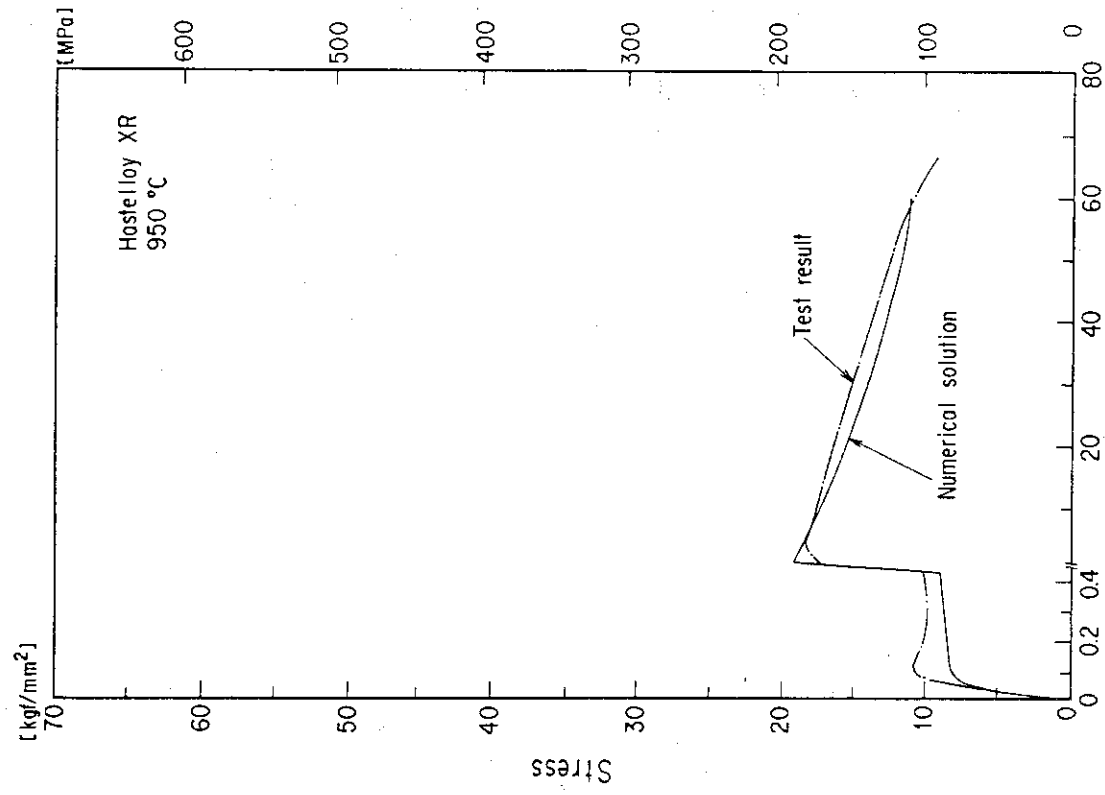

(c) For test temperature of 950°C

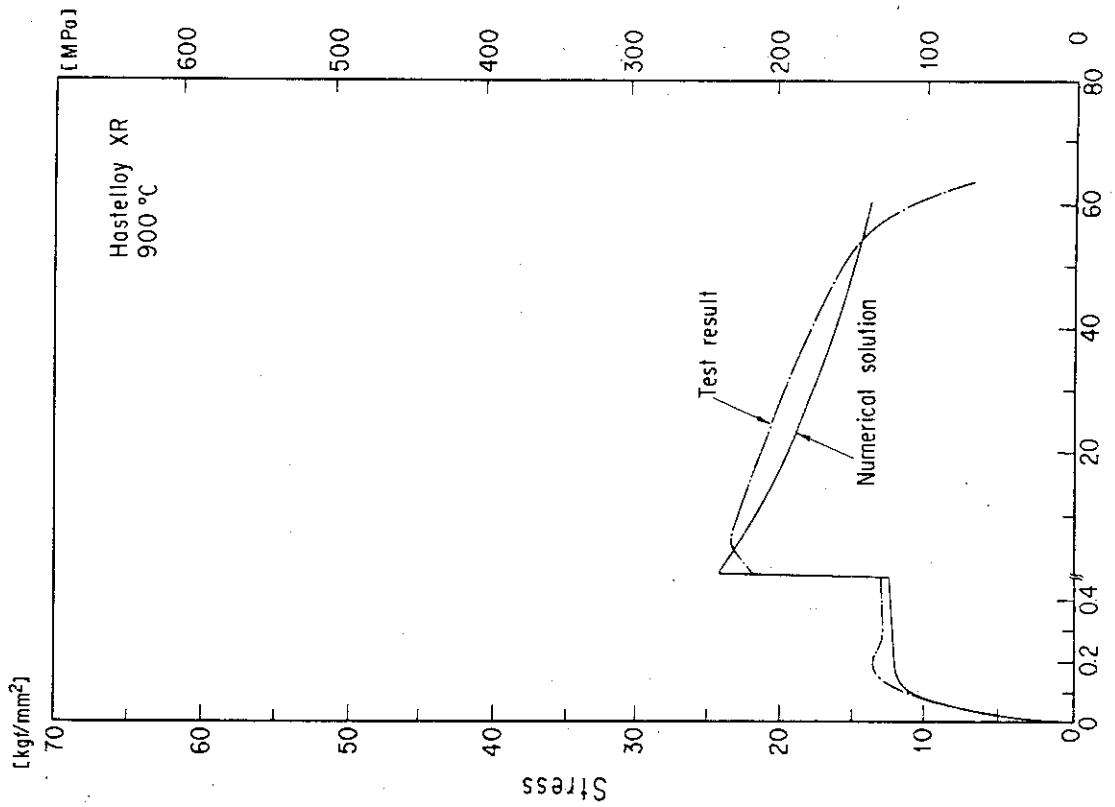

(b) For test temperature of 900°C

Fig. 21 Tensile stress-strain curves obtained by numerical analysis

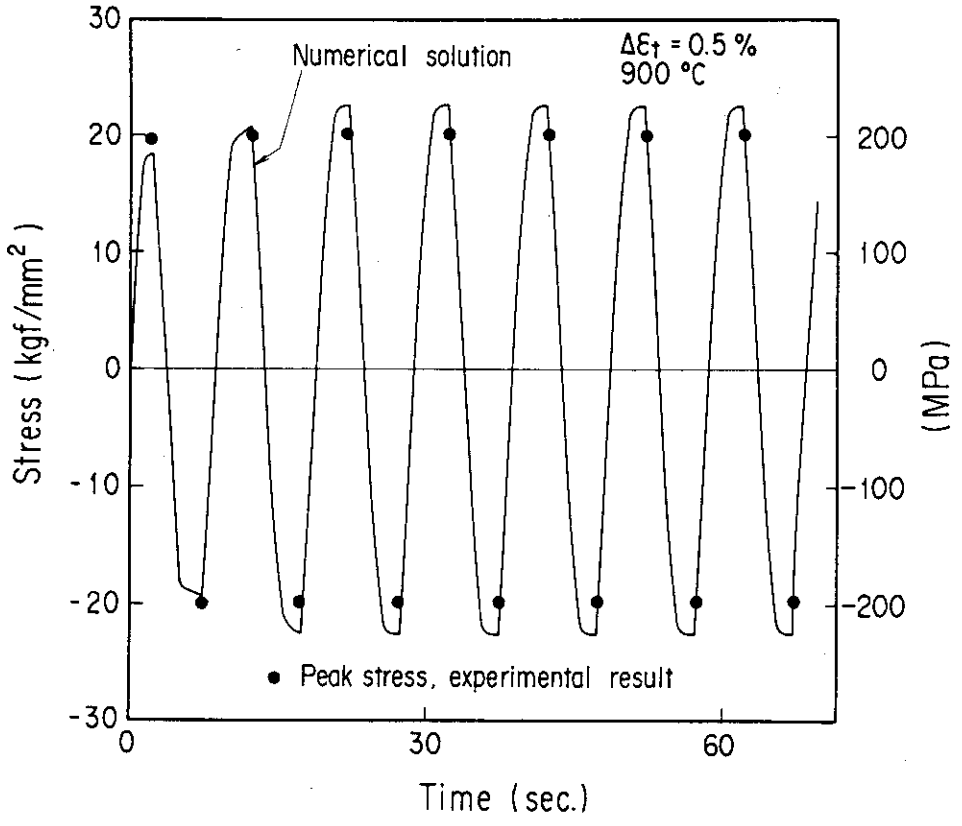

(a) For test temperature of 900°C under $\Delta\varepsilon_t$ = 0.5 %

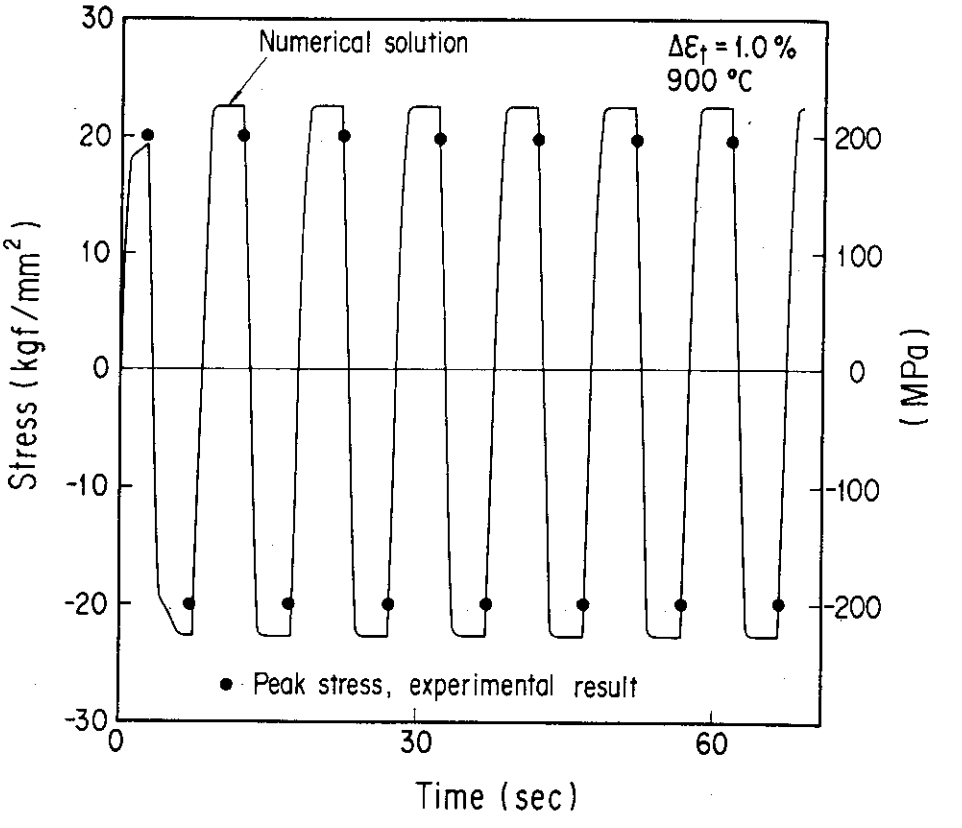

(b) For test temperature of 900°C under $\Delta\varepsilon_t$ = 1.0 %

Fig. 22 Time variation of stress during cyclic straining obtained by numerical analysis

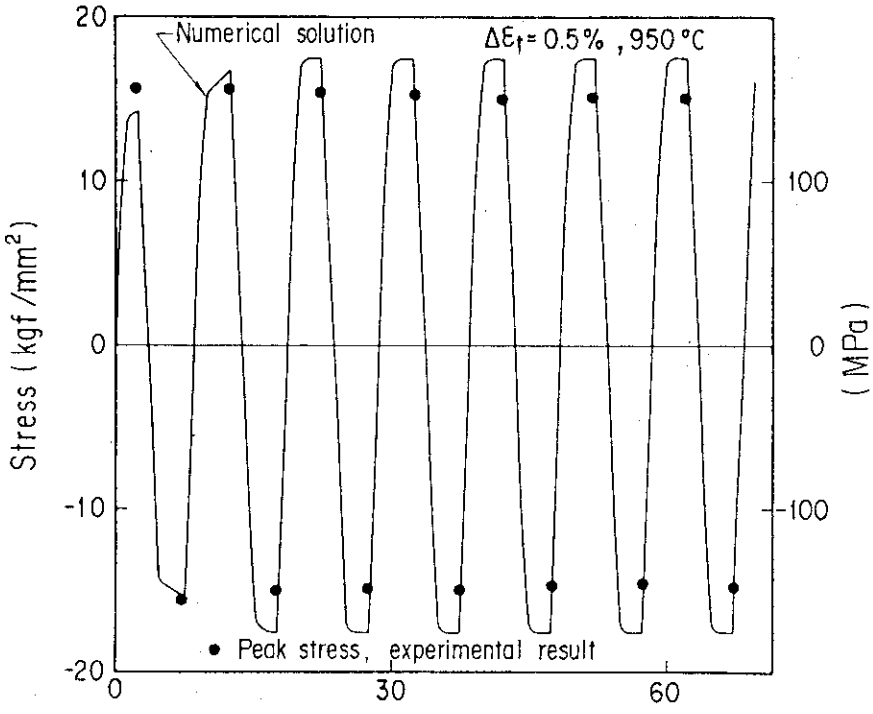

(c) For test temperature of 950°C under $\Delta\varepsilon_t$ = 0.5 %

Fig. 22 Time variation of stress during cyclic straining obtained by numerical analysis

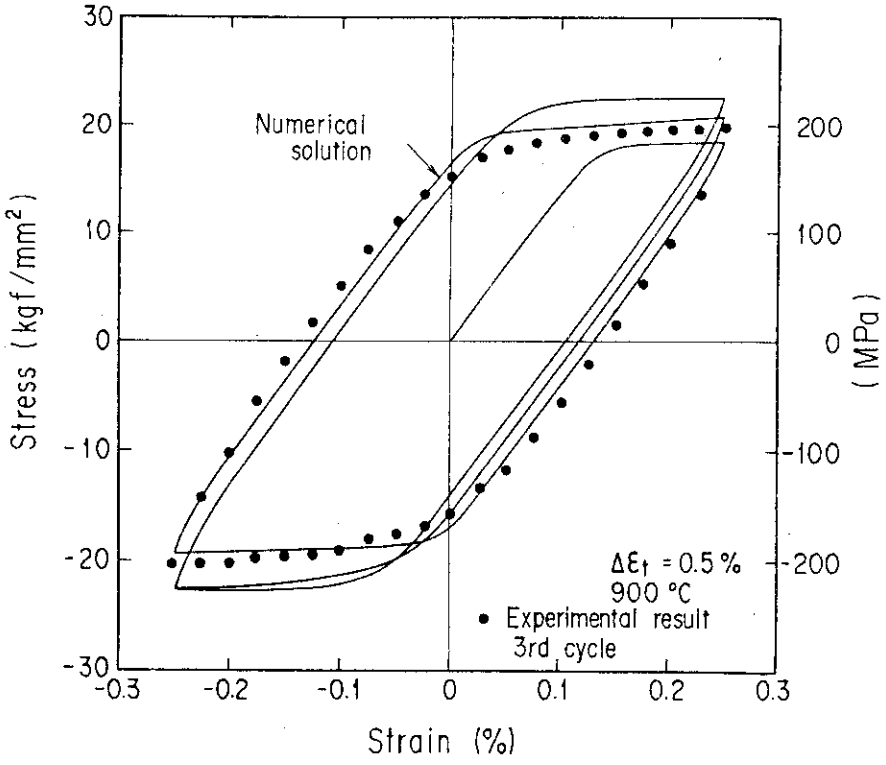

(a) For test temperature of 900°C under $\Delta\varepsilon_t$ = 0.5 %

Fig. 23 Hysteresis loop under cyclic straining obtained by numerical analysis

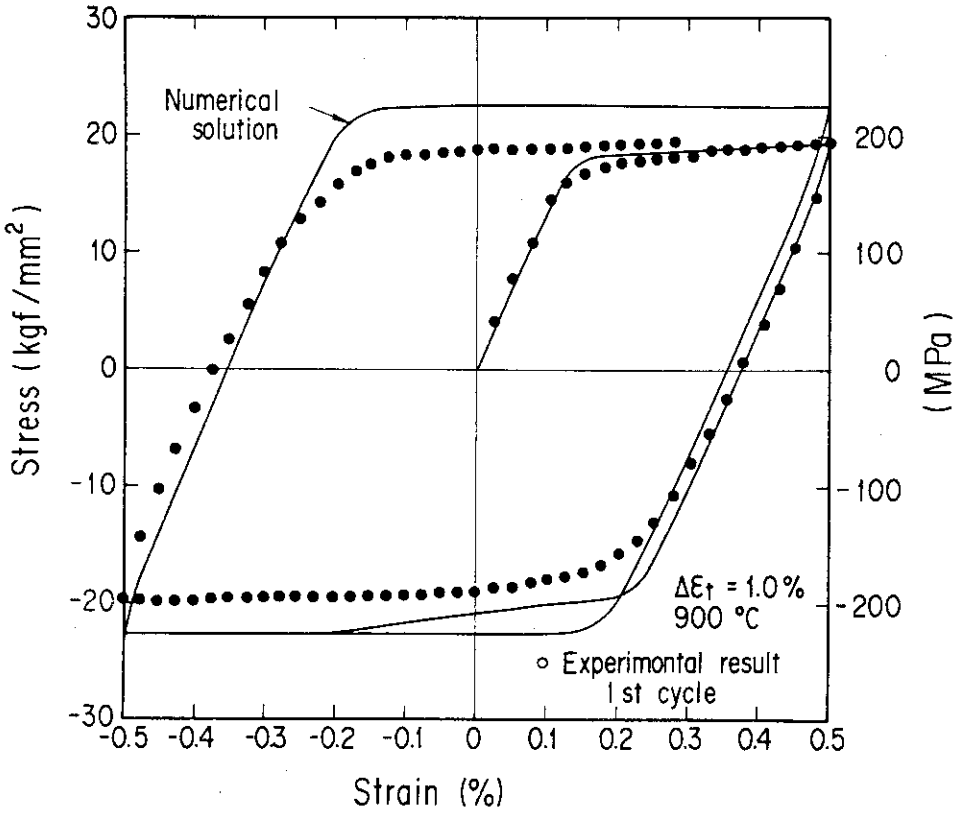

(b) For test temperature of 900°C under $\Delta\varepsilon_t$ = 1.0 %

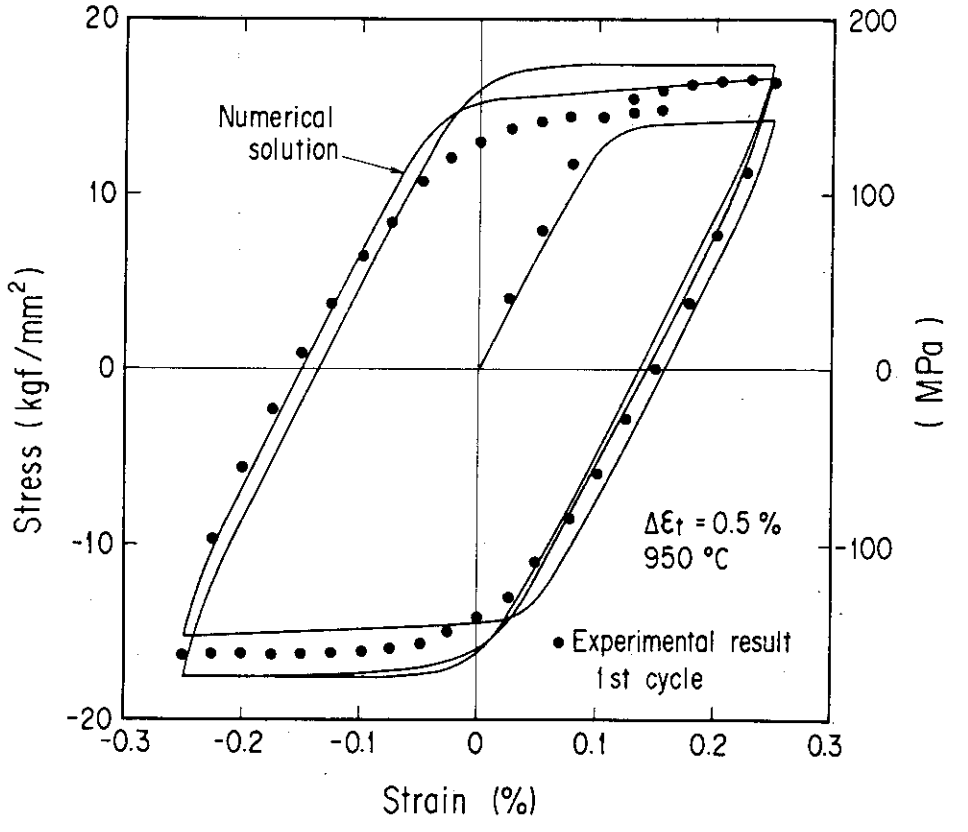

(c) For test temperature of 950°C under $\Delta\varepsilon_t$ = 0.5 %

Fig. 23 Hysteresis loop under cyclic straining obtained by numerical analysis